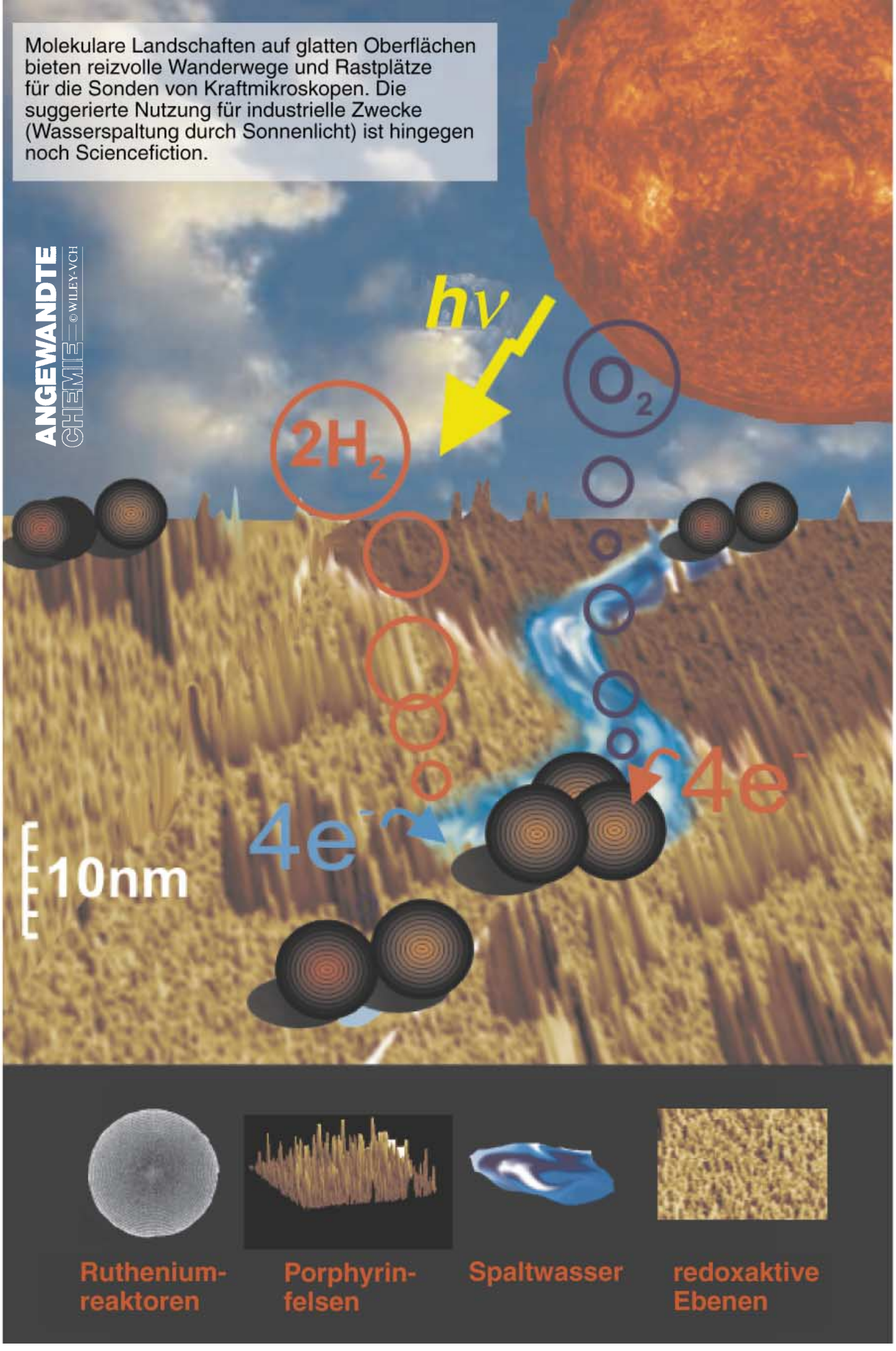
Molekulare Landschaften auf glatten Oberflächen bieten reizvolle Wanderwege und Rastplätze für die Sonden von Kraftmikroskopen. Die suggerierte Nutzung für industrielle Zwecke (Wasserspaltung durch Sonnenlicht) ist hingegen noch Sciencefiction.
ANGEWANDTE CHEMIE © WILEY-VCH
hν
2H2
O2
4e⁻
4e⁻
10nm
Ruthenium-reaktoren
Porphyrin-felsen
Spaltwasser
redoxaktive Ebenen

Rigid Lipid Membranes and Nanometer Clefts: Motifs for the Creation of Molecular Landscapes

Guangtao Li, Werner Fudickar, Marc Skupin, Andreas Klyszcz, Christian Draeger, Matthias Lauer, and Jürgen-Hinrich Fuhrhop*

Amphiphilic lipids associate in water spontaneously to form micelles, vesicles, monolayers, or biological membranes. These aggregates are soft and their shape can be changed easily. They behave like complex fluids because they are merely held together by weak, nondirected forces. The most important characteristic of these monolayers is their ability to dissolve hydrophobic molecules in the form of freely movable monomers. The fluid molecular layers are not suitable to anchor the components of chain reactions. However, if the alkyl chains are replaced by rigid skeletons or if the head groups are connected through intermolecular interactions, the aggregates become rigid and their fluid solvent character is lost. The construction of chiral surfaces by synkinesis (synthesis of noncovalent compounds) and of enzyme-type surface clefts of defined size can now be carried out by using rigid lipid membranes. Monolayers and nanometer pores on solid substrates attain sharp edges, and upright nanometer columns on smooth surfaces no longer dissipate. Five examples illustrate the advantages of using rigid molecular assemblies: 1) Cationic domains of rigid edge amphiphiles in fluid membranes act as manipulable ion channels. 2) Spherical micelles, micellar helical fibers, and vesicular tubes can be dried and stored as stable material. Molecular landscapes form on smooth surfaces. 3) α,ω-Diamide bolaamphiphiles form rigid nanometer-thick walls on smooth surfaces and these barriers cannot be penetrated by amines. Around steroids and porphyrins, they form rigid nanometer clefts whose walls and water-filled centers can be functionalized. 4) The structure of rigid oligophenylene- and quinone monolayers on electrodes can be changed drastically and reversibly by changing the potential. 5) 10^{10} Porphyrin cones on a 1-cm^2 gold electrode can be controlled individually by AFM- and STM-tips and investigated by electrochemical, photochemical, and mechanical means. In summary, rigid monolayers and bilayers allow the formation of a great variety of membrane structures that cannot be obtained from classical fluid alkyl amphiphiles.

Keywords: membranes · molecular landscapes · nanostructures · self-assembly · synkinesis

1. Introduction

The spontaneous self-assembly of amphiphilic lipids in aqueous solution leads to small molecular aggregates such as micelles, planar molecular bilayers (Myelin figures), vesicles, or biological membranes. Such aggregates are soft and flexible and behave like fluids. This is still valid at higher concentrations when lipid aggregates associate to micellar tubes (hexagonal or cubic phases) or when they are attached to solid substrates (Langmuir—Blodgett (LB) layers). The fluid character is a consequence of the fact that only weak undirected forces (van der Waals forces, hydrophobic effects) hold the lipid aggregates together and keep the head groups apart.[1]

Nevertheless, the spherical and rodlike micelles and vesicles in water as well as the planar lipid monolayers on solid surfaces are structurally well-defined. The effect of these ultrathin lipid membranes is, however, limited to the solubilization of hydrophobic organic molecules in water, the modification of the surface properties of water and of solids, and the separation of trapped volumes of water from bulk water. The fluidity of the alkyl chains of ordinary amphiphiles and detergents gives rise to their ability to dissolve hydrophobic isolated molecules. At the same time, this fluidity hinders the construction of rigid molecular cavities, which would correspond to enzyme clefts. Chain reactions, which, for example, would allow photolysis of water by sunlight, cannot be realized with fluid membranes.[2, 3] The organic chemist who wants to create stable molecular landscapes,

[*] Prof. Dr. J.-H. Fuhrhop, Dr. G. Li, Dr. W. Fudickar, Dr. M. Skupin, Dr. A. Klyszcz, Dr. C. Draeger, Dipl.-Chem. M. Lauer
Institut für Chemie/Organische Chemie, Freie Universität Berlin
Takustrasse 3, 14195 Berlin (Germany)
Fax: (+49) 30-838-55589
E-mail: fuhrhop@chemie.fu-berlin.de

  1433-7851/02/4111-1829 $ 20.00+.50/0

architectures, and machines by combining synkinesis (e.g. of heterodimers with defined molecular distances)[2, 3] with self-assembly,[1] should avoid fluid components. Instead, nature should be imitated as closely as possible: form and function are established by rigid proteins, which incorporate extremely complex reaction centers for biological processes.

To incorporate effective reaction centers within the easily accessible molecular mono- and bilayers of amphiphilic lipids, the properties of fluid membranes have to be modified. One should prevent micellar spheres of flexible amphiphiles from decomposing into planar bilayers within milliseconds of their removal from water. Boundaries between different motifs (plain, hill, valley, pond) should not be smeared out beyond recognition by molecules in the border region. Form-stable modules, which arrange in a defined order to allow a directed sequence of events, are needed for the construction of molecular machines. Rigid molecules based on amphiphiles will only be possible if the repulsive hydration forces are overcompensated by directed binding interactions between the membrane-forming amphiphiles or if the flexible alkyl chains are replaced by rigid polyenes, arenes, or steroids. Rigid membrane structures on solid surfaces or colloids can then be arranged around functional molecules that lie flat on the substrate. The membrane structures can then combine the function of proteins (to anchor reactive centers) with the matrix function of the membrane. Water remains the bulk solvent. However, the self-assembly properties of the ultrathin fluid lipid membranes must be retained. Figure 1 summarizes some typical characteristics of fluid and rigid lipid membranes: a) if the repulsive interactions between the small head groups of the amphiphiles are replaced by (weak) hydrogen bonds of bulky head groups, the micelles will no longer decompose upon drying; b) vesicle membranes on solid surfaces will no longer collapse upon drying, if fluid hydrophobic chains are replaced by rigid polyenes; c) micellar and vesicular fibers will survive in a highly diluted solution and on solid substrates if they are stabilized by two parallel hydrogen-bond chains between secondary amide groups; and d) the nanometer clefts in monolayers on solid substrates are also stabilized by hydrogen-bond chains.

The binding forces between the head groups may cause the curved rigid membrane systems (Figure 1) to crystallize quickly in bulk water.[1] Only those nanometer clefts in anchored surface layers (Figure 1 d), which resemble the edges of microcrystals, have a chance to survive. Herein we describe methods to isolate highly curved dry micelles and vesicles, as well as first attempts to integrate redox-active molecular modules into rigid membranes through noncovalent interactions. We focus on systems with the following characteristics: 1) easily prepared; 2) the components and their distances can be modified; 3) analyzable with routine methods; and 4) producible in large quantities. These requirements are best fulfilled by using water as solvent in combination with self-assembling polymer or lipid systems. We limit this Review to rigid lipid systems, but occasionally mention parallel developments with amphiphilic block polymers and multiple layers of polyelectrolytes.

2. Formation of Domains

The smallest rigid membrane structures, the domains, are generated by polar binding interactions between dissolved guest molecules in the center of fluid lipid bilayers. Ordinary micelles are too small to serve as hosts for large domains, and they usually dissolve molecules as monomers.[4] Exceptions are nucleic bases with short alkyl chains which agglomerate to give heterodimeric base pairs as a solid core in the fluid environment of the micelle (Figure 2 a).[5] Micelles also proved to be suitable for the synthesis of macrocycles, for

Back: G. Li, C. Draeger, M. Lauer, J.-H. Fuhrhop; front: W. Fudickar, M. Skupin, A. Klyszcz (from left to right)

Prof. Jürgen Fuhrhop has been instructing at the Institute of Organic Chemistry of the Freie Universität Berlin since 1977. His scientific work covers metalloporphyrin radicals und their diamagnetic π,π′-dimers, the ring opening of metalloporphyrins with molecular oxygen to form formylbiliverdins, ultrathin vesicle membranes of unsymmetrical and chiral bolaamphiphiles, and the transformation of helical fiber aggregates into sheetlike structures by the addition of enantiomers (chiral bilayer effect). Among other publications, his work has been summarized in two monographs.[2]

Dr. Guangtao Li, Dr. Werner Fudickar, Dr. Marc Skupin, Dr. Andreas Klyszcz, and Dr. Christian Draeger are current co-workers. They produced and characterized the form-stable nanometer pores (Fudickar, Li, Skupin), porphyrin towers (Klyszcz, Lauer), and micelles (Draeger) discussed in this Review.

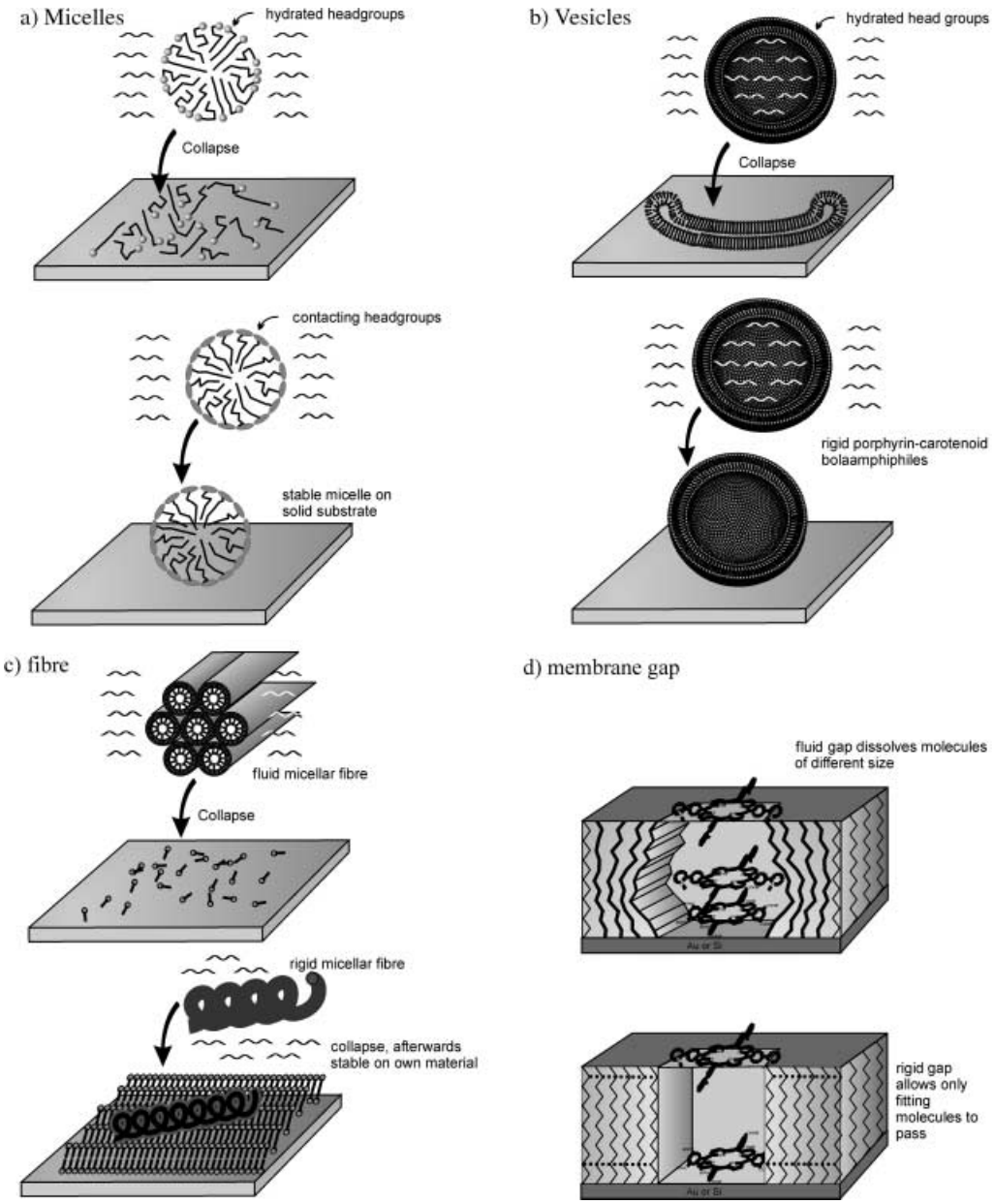

Figure 1. Comparison of fluid and rigid amphiphiles in a) micelles, b) vesicles, c) micellar fibers, and d) monolayers with nanometer clefts on smooth, solid substrates. Micelles and micellar fibers with a rigid head group area can be isolated. Fluid clefts in monolayers act as solvent, and rigid clefts act as filters and matrices.

example, porphyrinogens. Hydrophobic aromatic aldehydes and pyrrole form small aggregates that dissolve in micelles (Figure 2b). The shape of the micelle prevents the formation of large linear oligomers in the subsequent acid-catalyzed condensation. Instead, only small copolymers are formed. As soon as a cyclic porphyrinogen is formed, the reaction is interrupted. Oxidation with air leads to porphyrins; the average yield is 5–10 times higher than in homogeneous solutions.[6]

Polypeptide ion channels in biological cell membranes and synkinetic vesicle membranes occasionally consist of cavities in rigid protein helices (e.g. gramicidin S, Figure 3b), but mostly they consist of domains made of helical or linear edge amphiphiles (e.g. melittin, Figure 3a; see also Figures 4 and 5). The hydrophobic edge of these molecules dissolves in the membrane, the polar edges aggregate, attract water, and form pores. Positive electric charges at the hydrophilic edge seem to be essential to keep the edge amphiphiles at a distance, thus allowing ion transport.[7, 8] The alignment of the helices controls the ion flow: an inward-directed, negative membrane potential of 100–200 mV causes a higher cationic current when the dipole of the helix bundle is aligned in such a way that its positive end points to the outside. The bee poison melittin thus behaves like an adjustable edge amphiphile. First, it associates to the vesicle surface with its hydrophobic side and forms a helix with a strong dipole moment. Upon application of a membrane potential, it is integrated into the membrane.[7, 8] The hydrophilic surfaces are positively charged and form a broad ion channel (Figure 3a).[7]

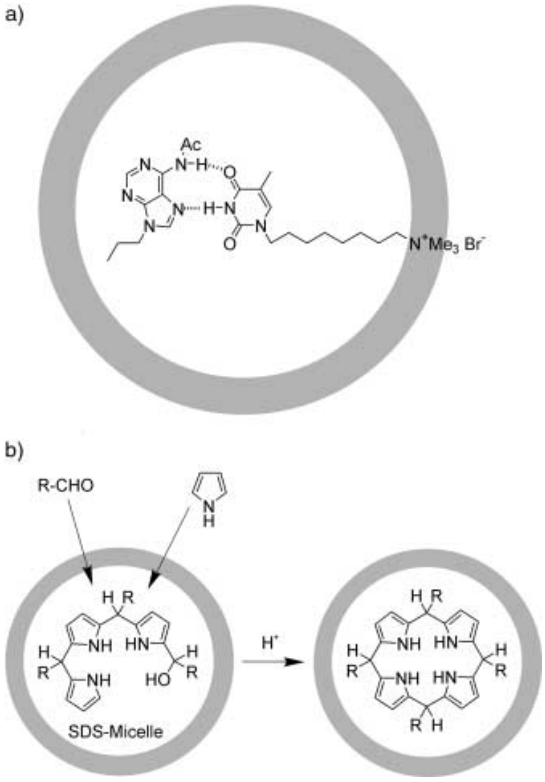

Figure 2. Fluid micelles are suitable a) to accumulate rigid hydrogen-bonded dimers, and b) as a trap for water-insoluble intermediates. In general, one only finds monomers in micelles. SDS = sodium dodecylsulfate.

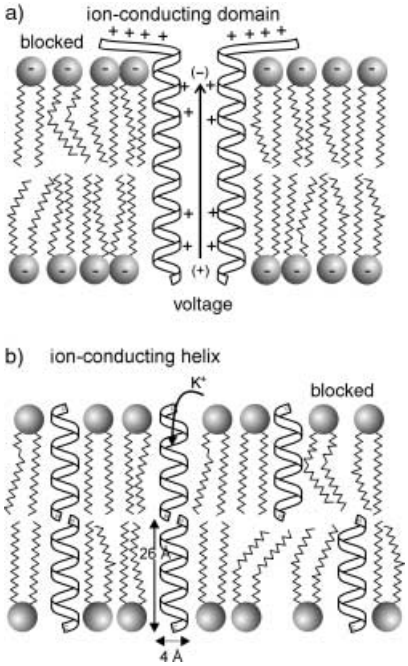

Figure 3. a) Domain formation of the helical edge amphiphile melittin leads to natural peptide channels in fluid lipid membranes. b) Alignment of two gramicidin helices in both halves of a lipid bilayer also produces rigid ion channels.

Helical protein edge amphiphiles occasionally also act as monomers or linear dimers without building domains. Gramicidin contains a hydrophilic cavity, whose diameter is large enough for the transport of potassium ions.[9–12] The gramicidin tube penetrates either the total double layer membrane by contracting it, or only half of an intact lipid bilayer. In the latter case, two gramicidin tubes must associate at their ends to allow an ion flow (Figure 3b). The relative mobility of two gramicidin helices towards each other is then necessary for the formation of the ion channel. If the inner and outer gramicidin helices are individually anchored by covalent bonds to a solid substrate, an ion current will no longer flow.[12] If, however, both helices are connected to each other covalently at the ends, the pore will be opened permanently.[11] In any case, the rigid membrane helix always migrates parallel to the alkyl chains of the membrane-forming amphiphiles. As the valine and leucine side chains fit perfectly within the fluid membrane structure, the helix does not leave the membrane nor does it form any domains that could disturb the fluidity and the impermeability towards ions.[9–11]

Not only water-conducting pores allow ions to penetrate through lipid membranes. Ill-defined edges of incorporated crystallites have a similar, though uncontrollable, effect. It was shown, for example, that a fluid vesicle membrane completely lost its osmotic activity, when carotenoid bolaamphiphiles had been incorporated. Borohydride and dithionite ions permeate the membrane within a few seconds along the edges of the hydrophobic crystallites, whereas the fluid membrane without crystallites constitutes a perfect barrier against ion transport.[13]

Real channel formation within defined domains or spacious helices can hardly be distinguished from membrane disturbances by current measurements with the patch–clamp method. Each pore should rather be defined as such by its ability to open and close reversibly. This can be effected by molecular plugs, light signals, modification of the pH-value, or other similar methods. Water runlets at the edges of crystallites would not give an "all or nothing" response to such a stimulus. With respect to artificial pores, reversible opening and closing procedures have so far only been demonstrated with oligoamine pores with carboxylate end groups. At pH 7, ethylenediaminetetraacetic acid (EDTA) acted as a plug. At pH 3, after neutralizing the terminal carboxy groups, it dissolved again in the bulk water, and the pore allowed the transport of ferrous ions (Figure 4). The positive charges of the ammonium groups on the hydrophilic surfaces of these edge amphiphiles clearly interacted with the carboxylate groups of the EDTA.[14]

Rigid tubes of cyclopeptide stacks were arranged vertically on gold electrodes (Figure 5), as proved by using small-angle FTIR spectroscopy ($I_{\perp} \gg I_{\parallel}$).[15, 16] The ability of the pore to be closed reversibly by plugs, has, however, not been demonstrated yet. Permeable boundaries between fluid membranes and crystallites or individual stacks could perhaps explain the permeability for ferricyanide ions just as well as the proposed ion channels made of domains of parallel peptide cylinders. Cyclic voltammetric studies of ferricyanide ions in bulk water did also not allow the determination of the exact mechanism of ion transport.[17] Patch–clamp measurements of the potassium transport through lecithin membranes showed considerable increases and decreases in conductivity; from these results one could deduce that opening and closing

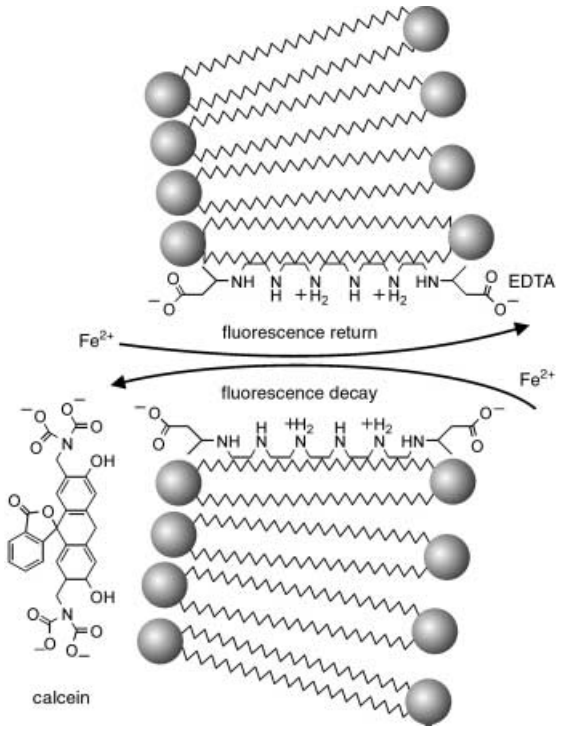

Figure 4. Closing and opening of a pore-forming domain by associating EDTA to a synthetic oligoamine edge amphiphile with terminal carboxylate groups. The penetrating ferrous ion extinguishes the fluorescence of the chromophore entrapped within the vesicle. EDTA in the bulk water withdraws the ferrous ions again.

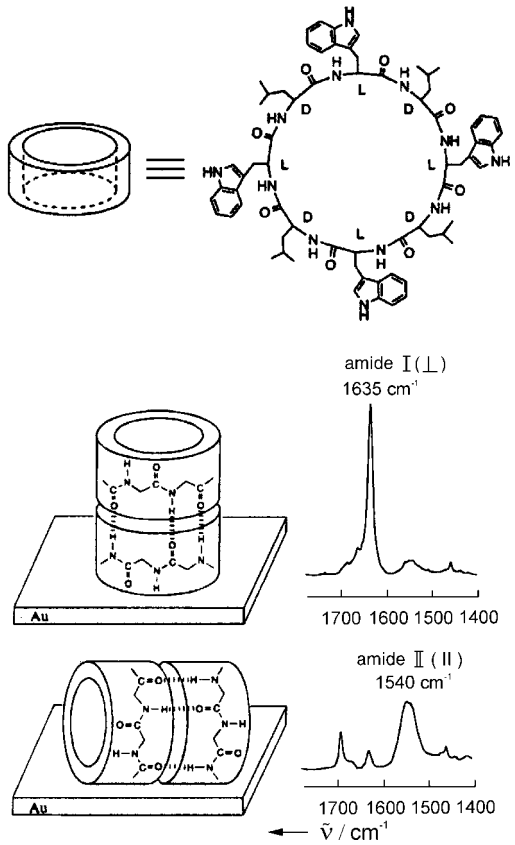

Figure 5. Cyclopeptide tubules can be arranged vertically or lie flat on a planar gold surface. Both positions can clearly be differentiated by FTIR spectra because the dipole directions of the functional groups drastically differ from each other in rigid aggregates.

operations are probably triggered by reversible dissociation of the staples.[18] Moreover, atomic force microscopy (AFM) measurements demonstrated that flat-lying cyclopeptide stacks arranged themselves vertically on glass when a lipid matrix was built up around them.[17]

The relative solubilities of amphiphiles either in the form of domains in fluid membranes or as micelles in bulk water are difficult to predict. Furthermore, edge amphiphiles tend to form complexes with metal ions. In general, rod-like polyol– or crown ether–oligomer edge amphiphiles do not directly transport metal ions through membranes, but accelerate potassium transport through valinomycin or proton transport along hydrogen-bond chains. It is remarkable that all these highly water-soluble compounds associate to lecithin membranes without any problem and presumably also span them.[8, 19, 20]

This applies similarly to the so-called electronic conductors or "molecular wires" made of the membrane-spanning polyene caroviologen, a carotene with a viologen head group.[19] Clear evidence of electronic conductivity through polyene molecules has only been obtained electrochemically, by two methods:[21a,b] 1) a gold-supported monolayer of β-carotene with thiol end groups produced a 10^6-fold higher conductivity to a tunnel microscope tip than an equally thick monolayer of alkyl sulfides, but its conductivity was, nevertheless, 10^4-fold lower than that of solid-phase polyacetylene;[20a] 2) the rate constants (k_{obs}) for the electron transfer from gold to ferrocene were measured as a function of the bridge lengths (in Å) of the alkane and phenylethynyl bridges.[21b] For the conjugated aromatic systems, a β value (β = linear inclination of $\ln k_{obs}/l$) of $-0.9\,\text{Å}^{-1}$ was measured, and for alkyl chains a value of only $-0.36\,\text{Å}^{-1}$ was found. A distance of $l = 20$ Å thus corresponds to an electron-transfer rate that is 10^{10}-fold faster in conjugated systems. The chemical Michael addition analogy of electrons "adding" to polyenes with carboxylate or pyridinium end groups and subsequent electron movement along the rigid "wire" is a plausible mechanism, but has presumably never been realized.

In one case it was clearly shown that ion transport through vesicle membranes occurred by translocation of ions along the "polyene wires" and not by electron conductivity.[14] Such proof will be possible, if the electron acceptor that is trapped within the vesicle, for example, an indigo dye, forms different products with different reductants: reduction with electrons should lead to a single product, regardless of the electron source.

3. Isolable Micelles and Vesicles

Micelles are molecular assemblies with the smallest possible diameter, that is, with the highest curvature of a molecular bilayer of alkyl chains.[1–4] This curvature occurs because the fluid alkyl chains, which have many *gauche* bends, are broader than the head groups and consequently push them wide apart. The head groups then bind a considerable amount of hydration water and are isolated from each other by repulsive hydration forces.[3, 4] If, however, the bulky head groups occupy the total spherical surface of the alkyl droplets and

if the cohesion of neighboring head groups are enforced by intermolecular hydrogen bonds, the hydrated water will partially be dislocated, the critical micellar concentration (CMC) will drop sharply, and the fluid micelles will become isolable as dry material.

The easiest way to enable contact between the head groups on a highly curved surface is to make them large. Bulky cationic head groups, especially those of trialkyl ammonium groups combined with large soft anions, lead to cationic micelles, which could be deposited on solid substrates with a negatively charged surface, for example on amorphous silica gel. Under water, 7-nm micelles or the corresponding cylindrical micelles were found by AFM.[22a,b] With even larger head groups, which have binding interactions with each other, spherical micelles were found that could even be isolated in the dry state. Kanamycin, a trisaccharide-like tuberculosis remedy with four amino groups, proved to be a suitable head group for this purpose. The surface of a sphere of 100 fluid octadecyl chains should measure about 12000 Å^2. The surface of a kanamycin molecule amounts to 75 Å^2. Consequently 150 head groups are sufficient to cover the surface of the micelle completely. Moreover, intermolecular hydrogen bonds between amino-, ammonium-, and hydroxy groups can displace most of the hydration sphere. Indeed, upon simple shaking, a C_{18} amide of kanamycin gave an aqueous micellar solution with a CMC of $< 10^{-5}$ M. A solution of these micelles (10^{-3} M) was applied to a carbon foil; transmission electron microscopy (TEM) showed the expected stable micelles with a diameter of about 6 nm (Figure 6a). AFM images of the same micelles on mica showed them as well-ordered stripes on the crystal planes of the substrate. The height of 5 nm corresponded to a molecular bilayer (Figure 6b). After applying a dilute solution (100 ×), the micelles did not lie side by side, but were isolated from each other, and dissipated over a molecular bilayer to semi-micelles. Both the densely packed micelles and the isolated semi-micelles

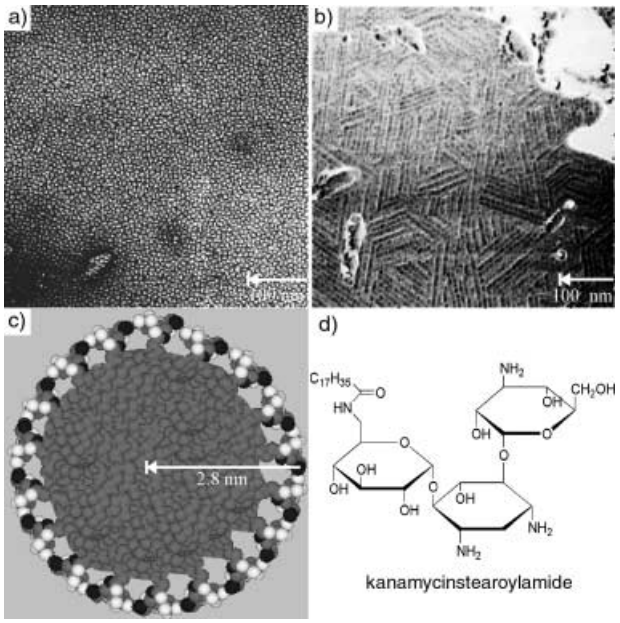

Figure 6. a) TEM and b) AFM pictures as well as the model of c) a kanamycin – stearylamide micelle.

remained stable for hours on solid surfaces in the dry state. In aqueous solution they behaved like fluid micelles and formed monomolecular solutions of metalloporphyrins.[23]

The concept of using large, interconnected head groups to make isolable micelles was also successful with metal complexes with two oligomethylene chains. Tris(bipyridinium) complexes of ruthenium with two C_{18} or C_{16} chains dissolved in water to form multishell micelles upon sonication (Figure 7).[24] However, these are micelles and not vesicles

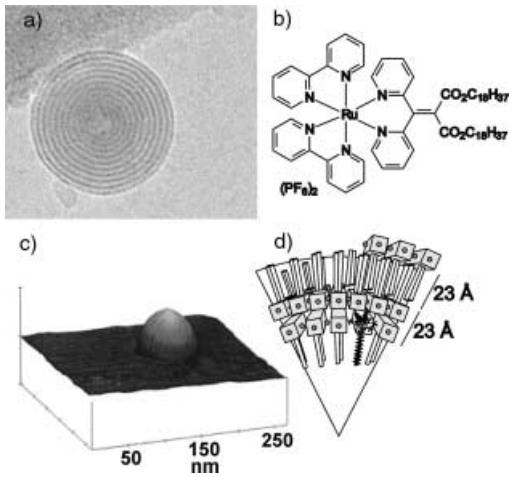

Figure 7. a) TEM pictures and b) structure of the monomeric tris(bipyridine)ruthenium hexafluorophosphate, c) AFM pictures of a micelle, d) model of a micellar fragment.

because no volumes of water are included by their membranes. The oligomethylene chains of the amphiphile form the core of the aggregate. The following forces are involved in the formation of micelles: 1) strong bonds between the ruthenium bipyridine dications and the hexafluorophosphate counterions; 2) van der Waals forces between interdigitated alkyl chains; and 3) (so far unique to micelles) back-to-back van der Waals forces between the head groups. The result is an assembly of spherical shells made of interdigitated double combs or herringbone patterns (Figure 7). The micelle can be isolated in the dry state and does not spontaneously associate as crystals of planar double layers, because the two highly organized, interdigitating oligomethylene chains do not allow reorientation of the head groups. These ruthenium micelles fluoresce and are photochemically active. If the rigid order of the double layers is disturbed, the fluorescence disappears. The corresponding palladium analogues form homogeneous micelles in water and have been utilized to catalyze Heck reactions.[25] AFM analysis has shown the $(C_{18})_2$–Ru compound in the form of undistorted micelles on gold and mica surfaces (Figure 7c). On graphite, however, the micelles were torn apart to form planar bilayers of flat amphiphiles.[24]

The C_{16} homologues are stable only on alkane layers. On graphite, mica, silica, and gold they spontaneously form three different configurations of planar double layers (flat-upright; head-to-head; head-to-tail; Figure 8). The most extensive decomposition of the micellar bilayer always takes place on graphite, because it strongly interacts with both the hydrophobic tails and the hydrophilic head groups. On mica, gold

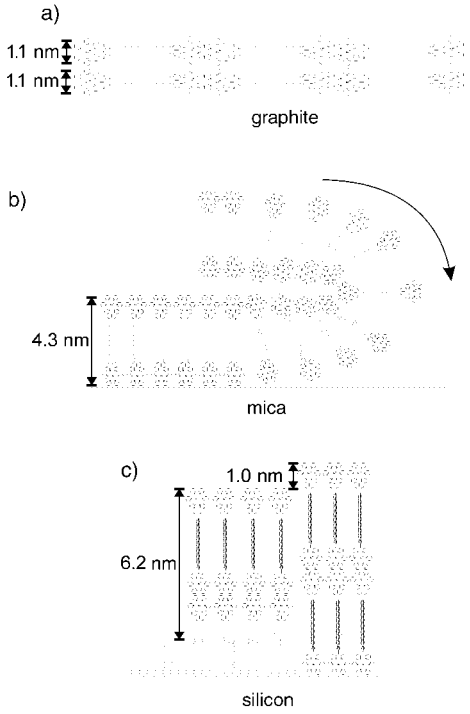

Figure 8. Model of the molecular configuration of bilayers, as they are formed on different planar substrates after the micelle has burst (see Figure 7).

and silica surfaces, the original interdigitated bilayer is maintained, only the curvature is lost.[26]

Spherical aggregates, which can be dried and stored, can thus be maintained by reversibly connecting head groups with a large surface area. The dominance of repulsive hydration forces does not necessarily lead to crystal planes upon drying. Water-free bi- and multilayered micelles are now available as isolable material, and it should be possible to load them with any monomer.

Isolable vesicles can generally only be obtained as covalent polymers. The first solvent-resistant polymeric vesicles with bilayered membranes were produced from vinyl groups in the head group region or at the end of the alkyl chains. However, nothing is known about the stability of these vesicles on solid substrates.[27–33] A large number of block polymers made of hydrophobic and hydrophilic subunits were synthesized; these block polymers formed spherical particles with an undefined membrane thickness and diameters of about 10–100 nm.[31–33] Those vesicles were loaded, for example, with colloidal palladium or rhodium and then used to catalyze Heck or hydroformylation reactions.[31a,b] Other polymer vesicles were used in toluene to optimize cryoelectron microscopy methodology.[33] Vesicles of noncovalently bonded cationic amphiphiles, which were solidified by cholesterol (50 mol%), proved to be stable on a cationic substrate and were characterized by AFM.[34] However, they remained stable only for a few minutes, before converting into planar bilayers.

Mono- or bilayered lipid vesicles without an included volume of water appear impossible at first sight: a free-standing 5-nm thick membrane should immediately collapse upon drying. Only one exception is known and is a result of the rigidity of the polyene amphiphile used, whose inner end had to be anchored to a rigid porphyrin carrier: eight α,ω-dicarboxycarotenoids (bixin) were attached on a porphyrin skeleton in such a way that four carboxy groups both above and below the macrocycle produced a bolaamphiphile with a large surface. The rigid polyene rods were arranged parallel to each other, and the porphyrins formed a rigid center. Spheres (40 nm, with 5-nm-thick walls) then formed in water and remained stable upon drying and on solid surfaces, even without covalent polymerization (Figure 9). The membrane is permeable to ions and therefore osmotically inactive and completely resistant to the addition of electrolytes.[35] After radiation with visible light, the polyene polymerized and the rigid vesicle became totally inert to organic solvents.

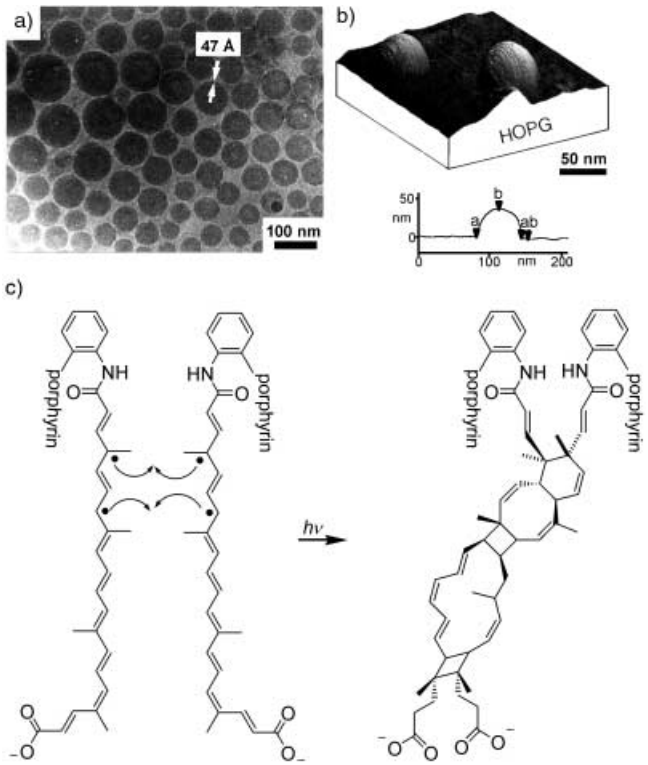

Figure 9. a) TEM and b) AFM pictures of the porphyrin–octabixin ester sphere with 4-nm thick walls; c) model of the light-induced polymerization. HOPG = highly orientated pyrolytic graphite.

An octabixinatoporphyrin is certainly not a useful amphiphile for general use. Thick-walled polyelectrolyte vesicles are also not promising transport systems for active substances in the human body. These rigid spheres can thus not compete with fluid vesicles (cyclodextrins and polymer microcapsules), which have proved to be effective transport systems.

4. Micellar and Vesicular Fibers

Amphiphiles with chiral head groups (glycon, amino acids) and secondary amide groups in the hydrophobic skeleton also form fluid, spherical micelles in water at temperatures above 80 °C. Upon rapid cooling of the aqueous solution, the

amphiphiles agglomerate to give extraordinarily form-stable, noncovalent fibrous micelles, which are frequently helical and can be isolated in the dry state. Quadruple helices, twisted ribbons, or tubular helices have been observed by TEM. The fibers are often very similar in appearance to protein fibers, which have been discussed in detail in a previous review.[36]

D-Gluconamides form isolable quadruple helices in water (Figure 10a, c), which convert into sheetlike structures and precipitate upon the addition of the L enantiomers (Figure 10b). This effect is of general importance for the stability of bioorganic gel and is called the chiral bilayer effect (Figure 10d).[37] This effect occurs in numerous amphiphiles with chiral head groups (for example, glycon,[37–39] glutamic acid,[40] and tartaric acid[41]) or with a chiral hydrophobic skeleton[42, 43] as well as for the helical polymer homopolylysine.[44] The pure enantiomers always form chiral fibers and stable gels in water. Upon the addition of the opposite enantiomer to the gel, crystallites precipitate and the gel is totally liquefied. In the case of gluconamide quadruple helices, which were isolated in the dry state and studied by solid-state ^{13}C NMR spectroscopy, the conformation of the head group was completely analyzed by comparing spectra of crystals of related open-chain carbohydrates, whose crystal structure was known (Figure 10e).[45, 46] A *gauche* bend near the outer end ($_2G^-$ conformation) of the head group was found in the fibers. This *gauche* bend is stabilized by a cyclic arrangement of hydrogen bonds and is responsible for the curvature of the fiber, because it makes room for hydration water, which enlarges the head group and promotes the curvature. Here, the formation of planar bilayers is prevented by directed hydrogen bonds and not by repulsive hydration forces. Recent experiments show that these well-ordered aggregates can be isolated as a dry material and preserved for years. Upon contact with solid surfaces they rearrange spontaneously to planar bilayers. The remaining fibers can then be deposited without any rearrangement onto the bilayers. AFM analysis shows them as "crests" on the plane. The solid substrate, for example graphite or gold, is located 5 nm below (Figure 10f).[47]

Other chiral amphiphiles form nonhelical bilayers, which roll up to multilayered tubes. Examples are D-mannonamide and D-galactonamide,[39] chiral alcohols from pine needles,[43] and bolaamphiphilic diamides with a lysine head group.[48] Lipid tubules made of bolaamphiphiles with an amino acid head group (e.g. lysine) and an amino head group are particularly easy to produce and handle. A slight variation of pH values produces homogeneous tubules of spherical vesicles and micelles (Figure 11).[48] The mannonamide fibers gave rise to hard, completely insoluble polymer rods when the diacetylene groups in the center of the bilayer were irradiated with ultraviolet light.[49] The gluconamide quadruple helices with their extremely high curvature disintegrated under identical polymerization conditions to ill-defined single strands.

Micellar fibers are consistently formed upon contact with solid substrates, for example, in the case of achiral 2-octadecyl-*p*-quinone-5-sulfonate, which is used in photographic layers. The amphiphile forms a stable monolayer on water; upon transfer to mica, the planar layer rearranges to form a lattice of micellar fibers, which are ordered side by side and have been resolved laterally by atomic force microscopy (Figure 12).[50] A strong interaction between the mica substrate and the quinone head group seems to be responsible for this fiber formation and not for its destruction. Although this

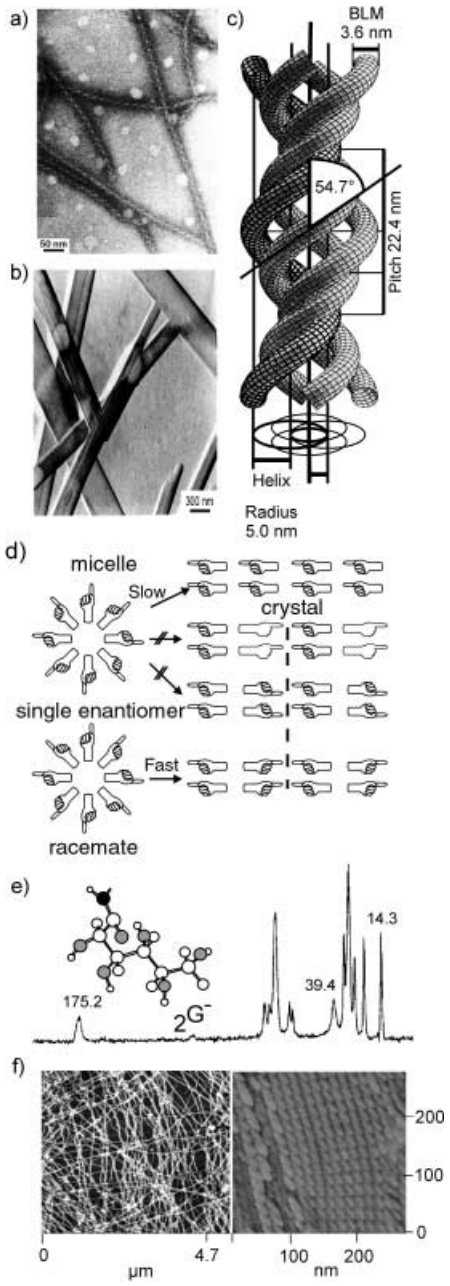

Figure 10. a) TEM of the micellar quadruple helix of *N*-D-octylgluconamide and b) of the racemate of both enantiomers. c) Model of the cross-section of a quadruple helix of a chiral amphiphile (BLM = bilayer micelle) and d) of the three corresponding crystal planes. Top: the head-to-tail arrangement corresponds to the most stable 3D crystal. Middle and bottom: two bilayers, in which the right- and left-handed chiral head groups are arranged differently. Such crystals are unstable and can usually not be isolated. The formation of the stable crystal (head-to-tail) needs a reorientation of the micellar bilayer and is therefore very slow in water. The micellar fiber remains stable for a long time. However, a spherical micelle from a racemate crystallizes rapidly upon cooling as a symmetrical bilayer. The micellar fiber is therefore short-lived. e) solid-state ^{13}C NMR spectrum of the fiber. f) AFM of the solid fibers.

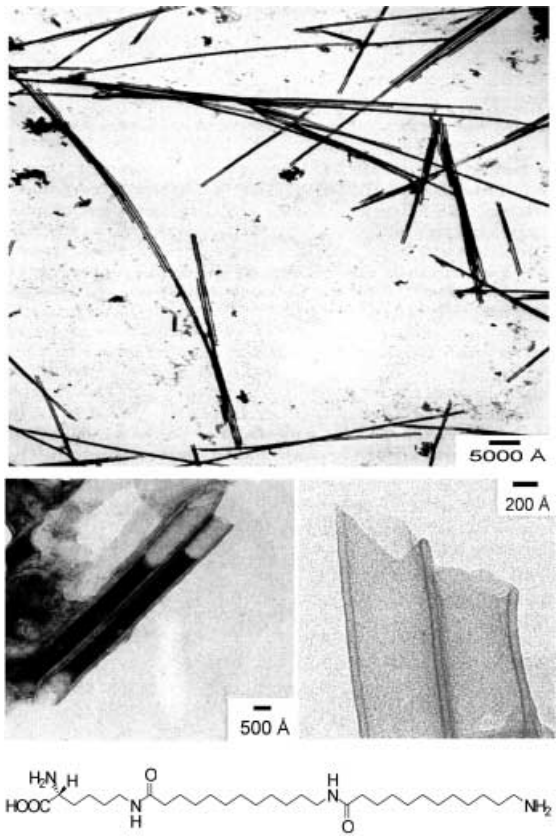

Figure 11. Vesicular tubules of a α-lysine-ω-aminobolaamphiphile.

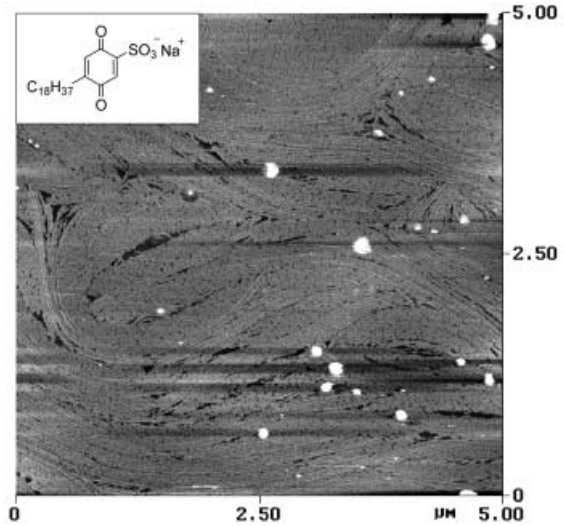

Figure 12. TEM of micellar 5-octadecyl-*p*-quinone-2-sulfonate fibers on mica.

phenomenon has not yet been explained, it is likely that the quinone sulfonate group plunges vertically into the water surface, but lies flat on the mica surface. The highly enlarged molecular surface of the monolayer promotes the transformation into a bilayer. In the present case, the repulsion between nonhydrated negatively charged sulfonic acid groups favor micellar fibers instead of planar interdigitated bilayers.

The flexible oligomethylene chain of the fiber-forming amphiphiles can be replaced by rigid porphyrins.[51–54] A suitable crystal of the amphiphilic protoporphyrin IX for structural analysis has not yet been obtained, although about 1600 porphyrin crystal structures are known, for example, that of the protoporphyrin dimethyl ester. Protoporphyrin itself is not among them because it forms fibers in water and other polar solvents, but not well-defined crystals. We suggest that this behavior applies to almost all natural products that appear in biological organisms in larger quantities: hardly any of the water-insoluble amphoteric natural products (e.g. fatty acids, carotenoid acids, biogenic amines, membrane proteins) crystallize spontaneously. Crystals are avoided, because they may clog capillaries and destroy the osmotic activity and fluidity of membranes. Cholesterol is an exception: it crystallizes from lipid fractions (this property gave steroids their name: stereos = solid) and is responsible for the damage caused by cholesterol in blood vessels.

Fibers with many different head groups were obtained from amphiphilic protoporphyrin derivatives. In the case of chiral head groups[52] or chiral axial ligands[53] their optical spectra showed very strong circular dichroism (CD) effects, whereas exciton effects and aggregate-specific fluorescence bands were not observed. This contrasts sharply to planar porphyrin platelets[55, 56] and fibers of amphiphilic polymethine dyes[57] (Figure 13), all of which fluoresce strongly. Some of the

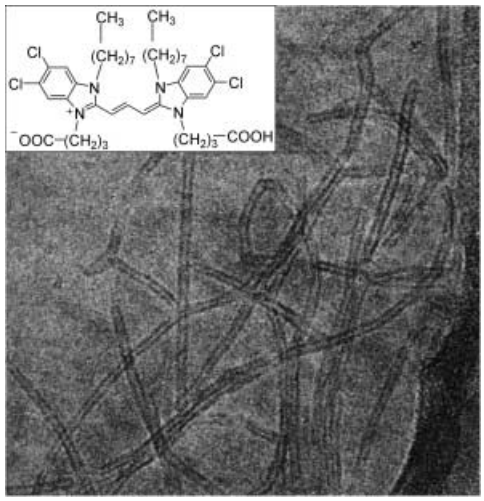

Figure 13. TEM of an energy-conducting fiber of the indicated methine dye.

polymethine dye fibers are stable in solvents as well as on solid surfaces. The thickness of their layers corresponds to a molecular bilayer, whose inner cavity has a diameter of about 1 nm. These assemblages were detected first by Scheibe[58] and Jelley[59] because of their extremely sharp fluorescence band, which is not common with monomers. Furthermore, these fibers and many monolayered porphyrin platelets show very large exciton effects, that is, the main optical absorption bands split up into two bands because of dipolar interactions in the excited states of the dyes. Typical wavelength differences between the two absorption maxima range from 30 to 120 nm. The polymethine dye fibers are used as "sensitizers" in commercial photographic layers and help transfer light energy to silver chloride particles. The extremely high photosensitiv-

ity of today's photographic films is partly a result of these fluorescent fiber aggregates.[60] The structural reasons for the sharp fluorescence band and the extreme exciton splitting of the aggregates, which seems to be necessary for an efficient energy transfer, was rationalized in theory,[61] but structural analysis of the molecular structures of the assemblies is still incomplete. TEM pictures of the fibers and platelets as well as the relative yields of fluorescence and exciton splitting merely suggest a positive correlation between the rigidity of the aggregates and their effective energy transfer. Optimization of the molecular interactions, which lead to energy-conducting material, remains an empirical venture.

5. Rigid Monolayers and Form-Stable Nanometer Clefts on Smooth Substrates

In the following section we limit the expression "molecular landscapes" to profiles on smooth surfaces of solids in the height range from 0.5 to 20 nm. In general, only the usual classic smooth solids are used in scanning force microscopy (SFM), namely graphite, gold and similar precious soft metals, as well as mica, quartz, silicon, and polymer films. On rougher substrates, <5-nm landscapes are hardly visible by STM or SFM. Since metal surfaces are the materials best suited for electrodes, gold (Au(111) surface) is most frequently used as substrate. Even quartz balances are first modified by covering the oscillating quartz with a thin gold layer and afterwards with receptor-active lipid monolayers.[62]

We start with polar molecules, which are deposited parallel to smooth surfaces. The classic example is guanine, which forms 3-Å thick monolayers on graphite upon self-assembly in 3×10^{-5} M aqueous solutions (0.1 M NaCl). When the surface potential is adjusted to $+80$ mV,[63] the guanine lies flat on the graphite grid and forms hydrogen-bonded aggregates. The guanine film between the positively charged electrode and a layer of chloride counterions remained unchanged at a voltage of 0 V. As the hydrated organic layer was then only a few Ångstroms thick, the electric field in the molecular plate condenser could be varied from -10^7 to $+10^7$ V cm^{-1} before electrolysis began. Such large variations in the field strength have an influence on the structure of the guanine monolayer. At a negative potential of -330 mV, the monolayer dissolved, whereas it formed again at $+420$ mV (Figure 14). At surface potentials of 80, 280, and 480 mV, rearrangements of the monolayer without detachment were observed by AFM. Although the formation, dissolution, and shape of the ultrathin 3-Å layer can be modified in many ways, it is totally stable at a given potential in the presence of bulk water.

Stable monolayers of flat-lying molecules were also obtained by the self-assembly of porphyrins. The simplest example is the *meso*-tetrakis(3,5-dicarboxyphenyl)porphyrin, which dissolves in water at pH 12 but nevertheless forms a stable monolayer on gold from such an aqueous solution. Presumably the carboxy groups interlock in subnanometer clefts on the gold surface, which form upon routine treatment with nitric acid, and are thus protected from deprotonation and hydration. After washing with potassium hydroxide

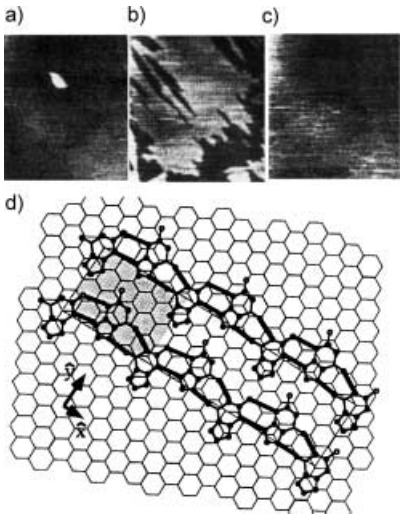

Figure 14. a)–c) AFM pictures and d) model of a guanine monolayer lying flat on graphite; a) the AFM picture at 0 and 420 mV shows a closed monolayer, which b) dissolves at -320 mV and c) re-forms at $+450$ mV.

solution, a porous monolayer remains in which the porphyrins adopt a Monte-Carlo arrangement (Figure 15; see also Figures 24 and 25). This implies that each porphyrin is bound in the place and orientation in which it arrives at the gold surface, that is subsequent rearrangements do not take place.

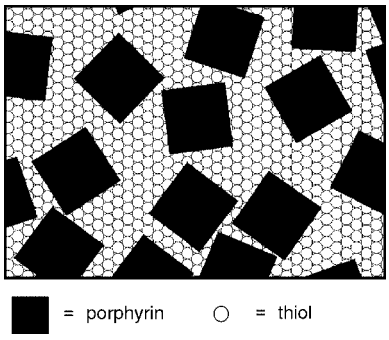

Figure 15. Model of the Monte Carlo arrangement of porphyrin molecules bound to gold after complete self-assembly. In a second step, a long-chain thiol is added to close the clefts (see also Figures 24 and 25).

The fluorescence yield of the porphyrin on such slightly rough gold surfaces is about 4–8% of that of the porphyrin on nonmetallic polyethylene surfaces. The addition of cationic porphyrin counterions with paramagnetic central ions quenched this fluorescence quantitatively and porphyrin heterodimers were observed on the gold surface. On a totally smooth gold surfaces ("mica gold"), the fluorescence was completely quenched, and the porphyrin carboxylates were not bound very strongly.[64]

Simple self-assembly from *n*-octylbenzene solutions allowed porphyrins with long alkyl substituents to be anchored in a flat and crystalline arrangement on graphite.[65] Such porphyrin monomers were still mobile after their adsorption to graphite. It is not clear yet whether this behavior is a result of the substrate smoothness or of the lack of polarity of the porphyrin. STM micrographs produced a perfect lateral resolution of the four pyrrole units and alkyl chains (Fig-

ure 16). Graphite surfaces bind equally strongly to polar head groups, aromatic compounds, and linear alkyl chains. As a result one usually finds only layers of flat-lying molecules (compare Figure 8). This behavior was not found on the amorphous carbon films used in TEM. In the latter case, most bilayers transferred from aqueous solutions survive without rearrangement.

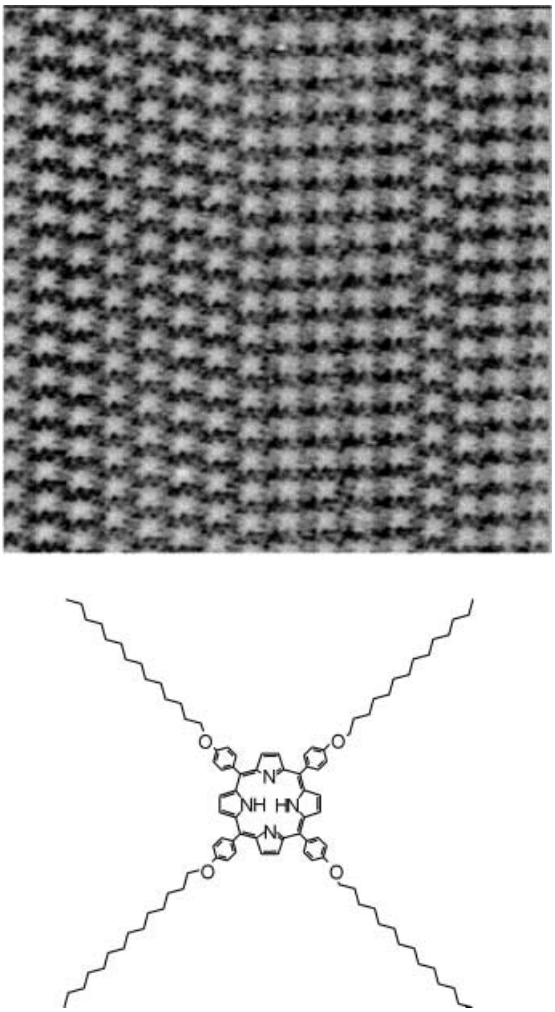

Figure 16. Perfectly resolved STM picture of a flat-lying crystalline layer made of long-chain (C_{14}) tetraalkyl porphyrins on graphite.

Steroids also bind in a flat orientation on gold when the binding thiol group appears in an axial position in the center of the sterol. The covalent Au – S bond forces the steroid into a position parallel to the gold surface. A suitable steroid for such flat monolayers is 7α-spironolactone. After self-assembly until saturation, about 50 % of the gold surface was occupied by steroids in a Monte Carlo arrangement; the remaining 50 % of the gold atoms remained unoccupied, as in the case of the octacarboxylatoporphyrin.[66] However, when 3β-thiocholesterol with a terminal equatorial SH group was used, the steroid molecules arranged themselves on the gold surface in a tilted, vertical orientation. The surface was covered quantitatively (Figure 17).[67] When ferricyanide was added to the bulk water, the electron current flowed freely through the flat-lying, porous membrane, whereas the vertically

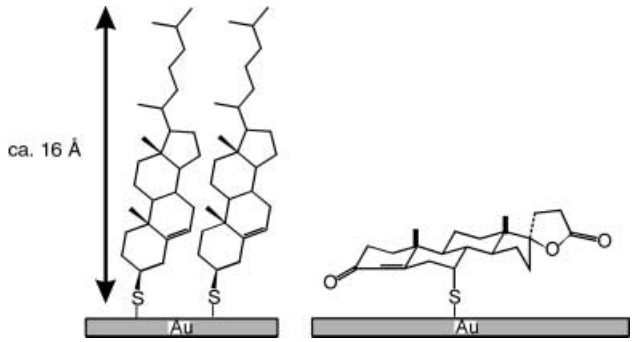

Figure 17. 3β-Thiocholesterol forms closed monolayers of vertically arranged molecules on gold; in contrast, 7α-thiospironolactone lies flat on the surface in a Monte Carlo fashion (see Figure 15).

arranged molecules produced a perfectly insulating 2-nm thick layer.

Thiocholesterol was our first example of a rigid amphiphile that forms impermeable, well-arranged monolayers on gold. Monolayers with fluid alkyl chains are arranged equally well in aqueous media. Their IR spectra show almost undisturbed *all-trans* conformations of the oligomethylene chains. As an example, cadmium arachidate monolayers are perfect insulators for ion currents and give rise to sharp Bragg reflections in neutron diffraction,[68] which means that the fluidity is lost in the 2D crystal, especially when bivalent cadmium ions solidify the basis. However, the oligomethylene monolayers become fluid upon contact with solvents, and their ordering is thus lost. Rigid rods, on the other hand, remain well-ordered, and the substrate thus remains "passivated" against attack from the surrounding bulk water.

Form-stable nanometer clefts as they are found on the surface of globular proteins do not occur in fluid membranes in water. A crystalline order only appears in the interior of the monolayers, not at the boundaries. This was shown in Sagiv's early experiments with dyes adsorbed to glass and surrounded by fluid monolayers.[69, 70] The dyes could be removed reversibly and introduced again; adsorptions and desorptions took place within seconds. Large dye molecules were also adsorbed, and size selectivity only determined the speed at which the adsorption took place.

Monolayers with cavities can also be created by the microwave-induced condensation of long-chained primary amines with surface-bound carboxylic anhydrides. The intermolecular cavities could be filled with alkanes (e.g. hexadecane or 1-octadecene). The IR spectra then indicated only *all-trans* chains. Weak dispersion forces between a fluid template and a fluid host clearly force the formation of a homogeneous *all-trans* conformation of the alkyl chains in aqueous media (Figure 18).[71] If the crystallinity of the alkyl chains in the hydrophobic areas is disturbed by inserting polar and/or large substituents (oxygen atoms, methyl groups) or slim rigid alkynes, the latter rearrange to form domains. Border regions are always amorphous. This is qualitatively valid for all mixed monolayers that contain rigidifying parts in the alkyl chain, for example, diacetylene[72] or sulfone dipoles.[73]

Several redox-active sulfides with rigid cycloalkane spacers are arranged vertically on the gold surface and allow charge transfer from the electrode to a distant electron acceptor and

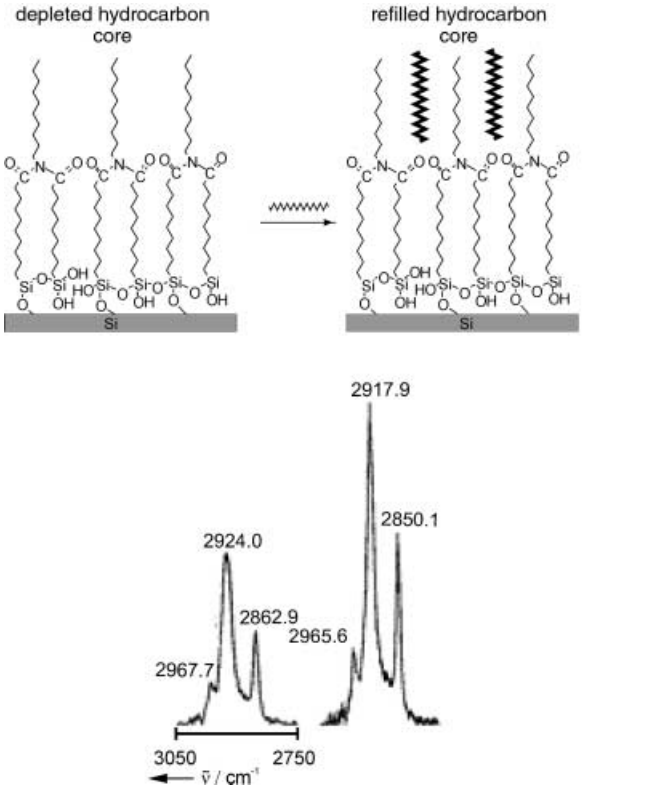

Figure 18. Rigidification of a porous fluid monolayer by adding equally fluid water-insoluble hydrocarbons such that the clefts are closed. IR spectra indicate flexible (left) and exclusively *all-trans* chains (right). For clarity, the alkyl chains have been shortened.

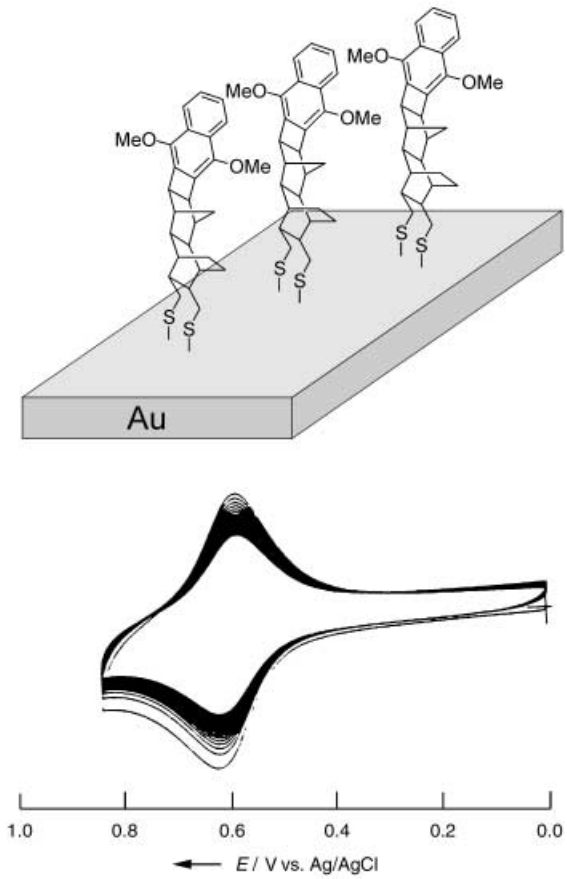

Figure 19. *O*,*O*-Dimethylnaphthoquinone, vertically bound on gold electrodes by a rigid skeleton, undergoes many redox cycles without being detached from the gold substrate. The sensitive Au–S binding is probably cleaved several times, but the reaction is reversed because the insoluble rigid molecule does not leave the surface of the electrode.

from an electron donor to the electrode. Dimethoxynaphthalene monolayers with a thioacetal substituent located far away from the quinone redox center were subjected several times to redox cycles of cyclic voltammetry. After 25 cycles, half of the original monolayer was still present[74] (Figure 19). The oxidation of the gold surface and the oxidative or reductive cleavage of the gold sulfide bond were essentially blocked. This is also true for multilayers of oligoimides (polymeric imides of naphthalene-1,4,5,8-tetracarboxyl anhydride)[75, 76] or staffane derivatives (oligomers of equally rigid bicyclo[1.1.1]pentanes)[77] with ruthenium(II) complexes located far away from the gold surface. An electron transfer across the Au–S bond was possible without reductive or oxidative cleavage of the Au–S bond, that is, the monolayer survived the redox cycles undamaged.

Complex but easily manipulable rigid membranes are accessible from amphiphiles whose hydrophobic portions are firmly connected to each other by hydrogen-bond chains. Secondary diamides are mostly used in analogy to protein sheets. Completely different end groups were anchored to gold surfaces by means of alkyl thiols ($RNHCOCH_2SH$). However, the monoamides do not offer a clear advantage over oligomethylene chains without functional groups.[8, 79] Rigidity only arises when two amide hydrogen bond chains run parallel to each other,[80] and both amide groups are located near the α and ω positions of a longer alkyl chain. Two neighboring amide groups do not induce rigidifying.[81] Well-insulating 2-nm layers were also obtained from combinations of monoamides with perfluorated end groups. The fluorine-substituted hydrocarbons not only act as perfect diffusion barriers and lubricants, but also keep the surface free from organic pollution (Figure 20)[82, 83]. Such monolayers are very efficient in protecting the Au–S bond.

The development of rigid monolayers that contain form-stable nanometer pores began with experiments on reactive diazido bolaamphiphiles on polyacrylamide (PAN). It was observed that two parallel chains of amide hydrogen bonds

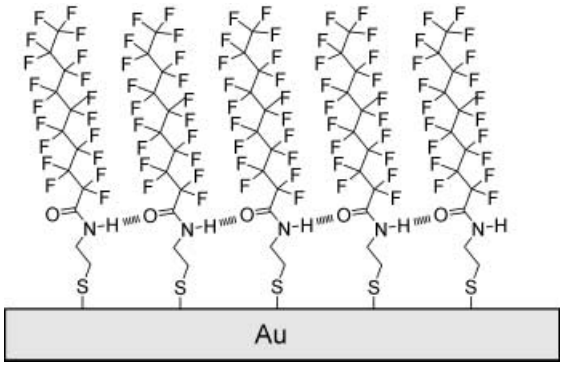

Figure 20. Double diffusion barriers made up of chains of amide hydrogen bonds and hydrophobic fluorocarbons protects the gold–sulfur bond from corrosion.

made the monolayer totally impermeable to methylamine, which is highly soluble in fluid membranes. The outer azido group reacted quickly, whereas the inner group was unreactive, even after several hours (Figure 21, left). A single amide group in the hydrophobic chain did not have any rigidifying effect.[80] On the other hand, two parallel chains of amide hydrogen bonds rendered the 15-nm monolayer impermeable, and an important odd–even effect was observed. This effect results from the angle of the alkyl chains with the substrate; parallel hydrogen-bond chains are possible if both amide groups form the same angle with the substrate (Figure 21, right).[84] This is only possible when there is an even number of connecting links between both amide groups. In the case of an odd number, there are nonpolar methylene groups located on both sides of one of the amide groups (not shown).[84]

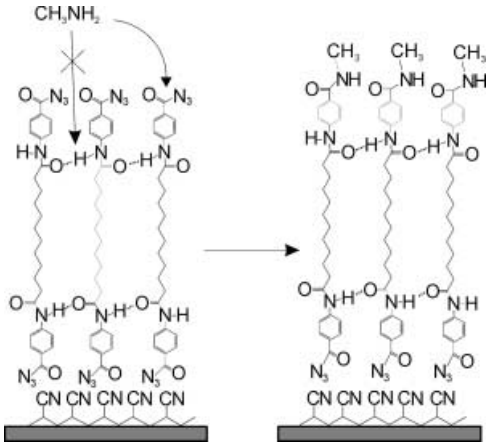

Figure 21. Left: a 15-nm lipid monolayer is totally impermeable to methylamine if two parallel amide hydrogen bond chains rigidify the monolayer; azide groups on the inside do not react with methylamine. Right: tilted monolayers of diamides remain fluid if the connecting carbon chain has an odd number of links; the monolayer is rigid with an even number of links.

A second method to solidify monolayers is to replace the alkyl chains by oligoarene derivatives, which also serve as light-harvesting antennae and as electron conductors. The simplest of this kind of layer gold consists of 4-methylthiophenol and is not thick enough to passivate the gold surface. Nevertheless, it protects the gold surface well from corrosion.[85–87] In contrast to toluene- or biphenyl homologues, phenylthiol hardly has any inhibiting effect on the transport of ferricyanide ions from the bulk water to the gold surface. Presumably, the unsubstituted phenyl rings are partly vertically orientated to each other, similar to benzene crystals, thus preventing the formation of insulating monolayers. Ferricyanide and ruthenium(II) salts in bulk water therefore produce almost undisturbed cyclovoltammograms (CVs). Substituted biphenylthiols are good insulators in most cases, but quickly decompose electrochemically or on exposure to oxidants. The self-assembly of a mixture of 4-nitrobiphenyl and 4-dimethylaminobiphenyl leads to an interesting selectivity: in the resulting monolayer the two components mixed spontaneously in a constant molar ratio of 3:2. With this ratio, the total dipole moment is reduced to zero, that is, the growing rigid monolayer rejects invading molecules if they polarize the monolayer too strongly.[88] STM micrographs of monolayers of substituted 4-thiobiphenyls showed ordered domains whose periodicity corresponded to the herringbone pattern of the crystal surface of biphenyl (Figure 22).[89] Terphenylthiol monolayers on gold were destroyed only very slowly by electrochemical and chemical oxidation. The rigid terphenyl layer acts as a good and stable insulator against the transport of ferricyanide ions to the electrode.[89]

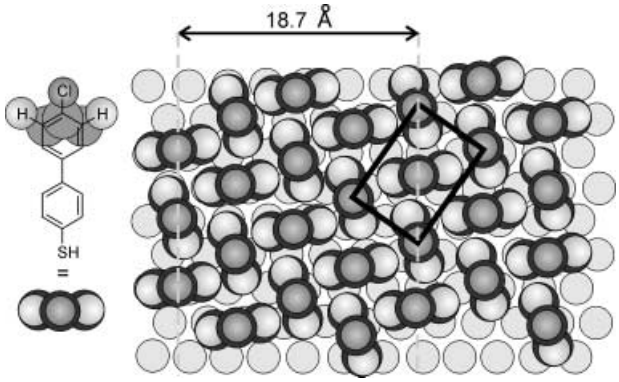

Figure 22. The herringbone pattern found in the crystal structures of biphenyl compounds is reflected in their molecular monolayers.

Rigid molecular arenethiol rods with connecting acetylene units gave heterogeneous, patchlike monolayers on gold,[90] whose clefts could only be closed by fluid thiols. In a second self-assembly step, hexadecanethiol partly substituted the rigid amphiphiles, closed the gaps, and led to perfect passivating monolayers. IR spectroscopic analysis revealed showed that the rigid rods still formed the main part of the membrane at the end of the self-assembly process. It is clear that isolated assemblies of rigid amphiphiles or small soluble domains are quickly substituted, whereas large blocklike domains remain upright.

The oligophenylene films on gold should conduct energy-rich electrons in cases in which they can produce anion radicals. A corresponding electrical conductor was actually characterized in mixed layers of acetylene-connected terphenylthiol and dodecanethiol monomers by means of STM. Each time the tip went over the 5-Å elevations of the rigid electron-rich domains on the dodecyl layer, tunnel current peaks of up to 40 Å were observed (Figure 23).[91] The effect here is much more distinctive than in the case of polyenes.[20]

The domains of rigid molecules in fluid membranes, of isolable micelles, vesicles, and fibers that have been discussed so far resemble those found in covalent polymers. However, they do not have covalent bonds, which survive drastic changes in external conditions such as rises in temperature, changes in pH, and attack from solvents. Proteins and nucleic acids, to name the best-known polymers that appear as micelles and fibers, also change their shape according to their environmental conditions, but they do not simply release their monomers. The molecular aggregates lack the robustness of the primary structure. In spite of this, will it be possible to mill clefts into the membrane structure, which correspond to the clefts in protein enzyme or to the grooves of nucleic acids? In principle, yes, if two rigid aggregates of different height are anchored successively onto a solid substrate. Conditions must

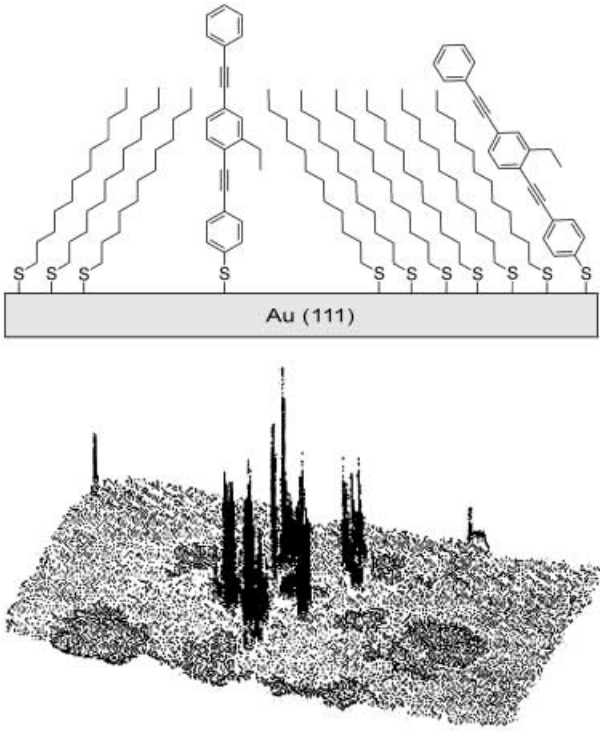

Figure 23. Scheme of a mixed monolayer of fluid dodecanethiol and rigid acetylene-linked terphenylthiol monomers; the latter act as electron conductors (1 V voltage of the electrode at 3-pA tunnel current); this leads to local current peaks (≈40 Å).

be chosen so that the substance applied first will not be substituted by the second, and that only unoccupied areas on the substrate will be occupied in the second step. At present, a two-step self-assembly of thiols on gold is the best procedure. The first substrate should shield its Au–S bonds efficiently and/or should be anchored by several Au–S bonds, which will probably not all be broken at the same time and will form again under mildly reductive conditions.

Porphyrin monolayers lying flat over about 50 % of the gold surface in a Monte-Carlo arrangement (see Figure 15) were surrounded with vertically arranged diamide bolaamphiphiles. Form-stable 2-nm pores formed around the porphyrin. A paramagnetic metalloporphyrin tetracation, which fitted perfectly into such a pore, extinguished the fluorescence of the porphyrin located at the bottom of 2-nm well within 30 min. A 10-Å broader porphyrin did not fit into and did not extinguish the fluorescence. This selectivity proves the desired rigidity of the pore walls. When a fluid membrane without amide hydrogen bonds was treated in the same way, no significant difference was found between large and small porphyrins (Figure 24).[64] Not only the size selectivity of the rigid cleft is remarkable but also its inaccessibility: the fluorescence in the fluid cleft is extinguished within a few seconds, whereas quenching requires 30 min in the rigid membrane. The relatively quick response in the adaptable cleft shows that the fluid membrane acts as solvent for the porphyrin cation. On the other hand, rigid tunnels allow heterodimerization only in the case of suitable porphyrins if the guest porphyrin diffuses spontaneously into the narrow tunnel. There is no long-distance driving force between positively and negatively charged porphyrins because the well is too deep to allow attracting ion–ion interactions between the upper opening and the bottom of the well.

Comparable diffusion processes are found in porous minerals, but rarely in biopolymers or biomembranes as the clefts and pores (enzyme clefts, DNA grooves etc.) are never deeper than a few Ångströms. Furthermore, the diffusion of metal ions through water-filled membrane pores along a concentration gradient has little in common with the diffusion of individual molecules in monolayer clefts.

Hydrophilic groups can be introduced on the rigid walls of the well without destabilizing them. C=C double bonds that are incorporated in the alkyl chains of diamide amphiphiles can be aminated by amines that migrate into the water-filled cleft. At pH values under 7, a cyclic arrangement of ammonium groups is formed at which a second anionic porphyrin can be anchored at a distance of 20 Å (amine formation the edge of the well) or 8 Å (amine formation in the interior of the wall; Figure 25).[92]

Porphyrin heterodimers with an intermolecular distance of 8 Å are promising systems for studying light-induced charge separation between electron donors (e.g. zinc porphyrinates) and electron acceptors (e.g. tin(IV) porphyrinates). Anionic quinones, flavins, and other redox partners can also be anchored to the ammonium rings by reversible salt formation. Addition of a base neutralizes the amino groups so that the anchored anionic electron acceptor is released into the bulk water. Fresh acceptor molecules can then be reinserted into the cleft, which means that bleached dye molecules are regenerated. The built-up charge can be neutralized by oxidants on the water side or by the electrode on the metal side. Connected systems may thus be established which split water with the aid of sunlight to hydrogen and oxygen.

6. Molecular Plateaus and Towers

The nanometer clefts in lipid monolayers described above are not suitable for electrochemical experiments with AFM or STM tips, as the clefts are too small to be detected by the tips. Noncovalent synthesis, synkinesis, can be used to construct towers of redox-active molecules on smooth substrates. Such objects are attractive, because they can be controlled individually by the AFM or STM tip and because they provide a great variety of objects for analysis. If, for example, only 10 tower-like nanometer-sized objects are anchored on an area of $100 \times 100\ nm^2$, then ten billion towers will be present on an area of $1\ cm^2$. Each individual object may allow experiments concerning photochemical conductivity, destruction by photochemical oxidation, recognition experiments with coated tips, etc.

The most important method to build up elevated objects on flat substrates is contact-printing with polymer stamps. This technique has a resolution of about 100 nm,[93] which is far above the dimensions discussed in this paper. Nevertheless we

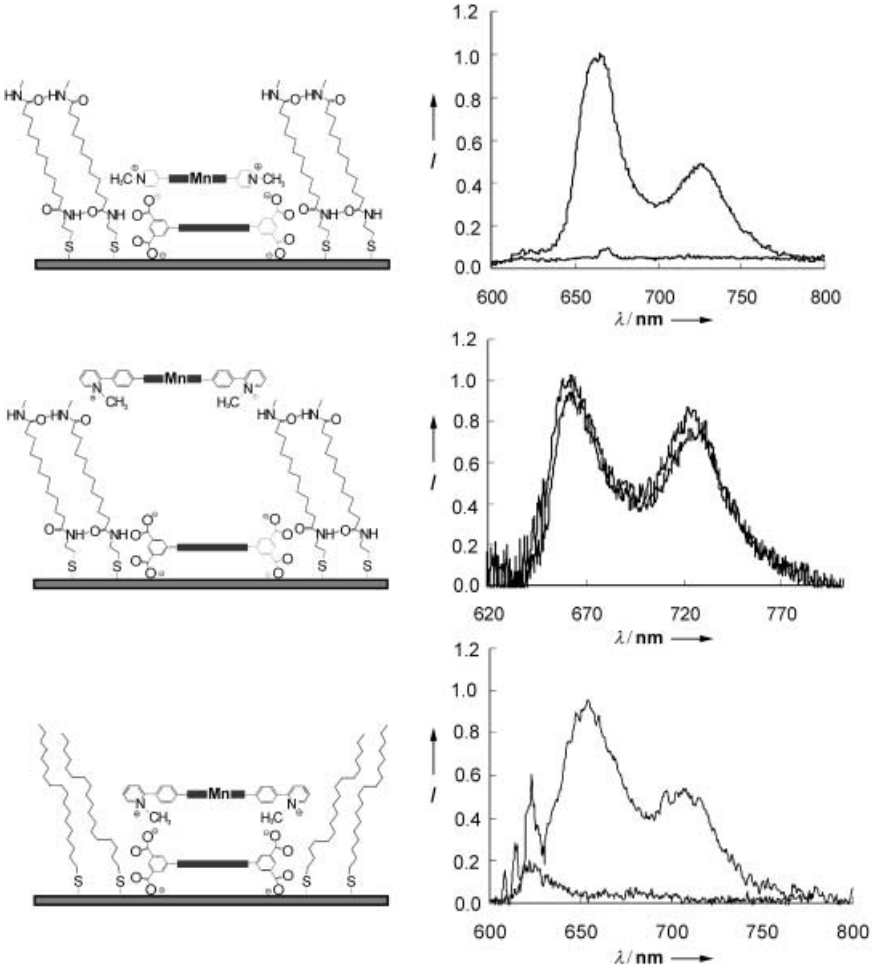

Figure 24. Porphyrins (20 Å wide) form close heterodimers in rigid membrane clefts, as indicated by the quenching the fluorescence (top). Porphyrins (30 Å wide) cannot penetrate into the rigid cleft (middle), but can do so into a fluid cleft (bottom). I = fluorescence signal, normalized for $I_{max} = 1.0$.

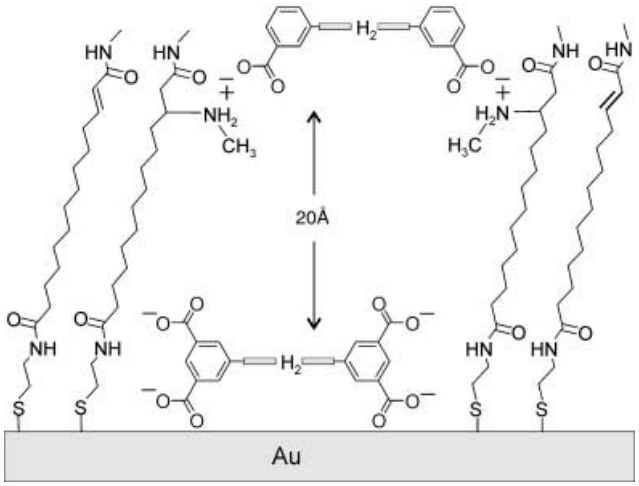

Figure 25. Noncovalent heterodimers of porphyrins that are anchored in a 2-nm-wide membrane cleft by functional groups at the walls at a defined distance (here: 20 Å).

discuss briefly the "inks" applied. For example, if alkane thiols are used on gold, the ink molecules will diffuse the edges are smeared. Palladium complexes and proteins, however, hardly move on the gold surface and therefore produce pictures of the stamp pattern that are accurate to a few nanometers.[94] Again we are clearly dealing with rigid objects and consequently an unmovable link between monolayer and substrate.

Rigid domains within a fluid molecular monolayer were produced from β-pyridinium-β-ethylporphyrin sheets and eicosanoic acid by using the LB technique. The porphyrin aggregated both in bulk water and on the water surface to form monomolecular sheets, which were characterized by a strong exciton splitting of the Soret band (λ_{max} 405 nm $\rightarrow$350 and 450 nm) and by intensive fluorescence bands (λ_{max} 620 and 730 nm).[55, 56] AFM images of these monolayers taken in the tapping mode showed, at first, closely ordered inclined eicosanoic acid molecules (h = 24 Å) as well as upright porphyrin molecules (h = 18 Å). Upon further tapping of the mixed monolayer with the AFM tip, a large number of the fatty acid molecules became vertically orientated to give 30-Å high peaks (singularities) in the 24-Å plane of sloping molecules (Figure 26). These singularities were long-lived (>7 days) even though they were located in the fluid part of the monolayer.[95]

It is rather easy to produce well-defined porphyrin multilayers from tetracationic and tetraanionic porphyrins. A particularly homogenous multilayer of this kind is composed of *meso*- tetrapyridylporphyrins with four peripheral ruthenium(II) complexes and *meso*-tetraphenylsulfonatoporphyrin.[96] The stepwise construction of isolated porphyrin towers suited for SFM experiments, however proved to be more difficult. A promising method involved the use of bifunctional axial ligands to bind the porphyrin metal centers. In the case of zinc – pyrazine or zinc – 4,4′-bipyridine complexes, only large aggregates were obtained, because the binding constants were too small ($K_1 \approx 10^3\,\text{M}^{-1}$; $K_2 = 0.1\,\text{M}^{-1}$) to enforce rigid edges.[97] In linear copolymers of zink porphyrinate and phenylene ethyne units, which form complexes with gold-supported bipyridine molecules, better results were obtained. Netlike structures up to a height of 60 nm were produced in six steps in the self-assembly of porphyrinate polymers with bis(pyridyl)ethylene ligands and characterized by AFM. (Figure 27).[98] Analogous interdigitations in monomolecular fibrous structures have also been obtained by means of covalent oxygen bridges between the phosphorus centers.[99] Isolated porphyrin towers or rocks did not form.

Experiments with porphyrin octaphosphonates and zirconium(IV) salts on silicon wafers were more successful. At first, phosphonate groups were anchored to the silicon surface, and their polarity was then reversed with Zr^{4+} ions. Subsequently, a layer of porphyrin was deposited, their polarity was again

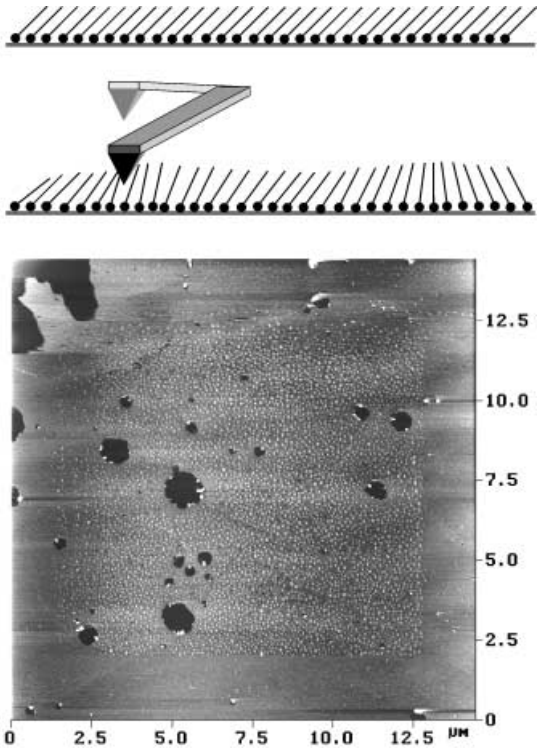

Figure 26. Model and AFM picture of long-lived waves (singularities; white areas) vertically arranged on a fluid membrane besides rigid porphyrin domains (black areas). The singularities are formed by AFM measurements in the tapping mode.

reversed with Zr^{4+}, and the procedure was repeated (Figure 28). This procedure is based on the finding by Alberti[100] that α,ω-bisphosphonate bolaamphiphiles with zirconium salts produce perfect single crystals as well as on the report by Mallouk and co-workers[101] on the self-assembly of regular layers of phosphonate amphiphiles on Cabosil colloids. Indeed, after establishing an appropriate capping procedure with the complex-forming Alizarin S, a landscape of isolated porphyrin towers with a maximum height of about 20 nm and a width of 4–6 nm was produced.[102] Alizarin derivatives, which are known to grow in the form of crystalline monolayers on smooth surfaces,[103] proved to be much better capping reagents than isolated single molecules, for example, *tert*-butylphosphonate. No slim towers were formed, but hard broadened cones were abundant (Figure 28); these were hard enough to be moved with an AFM tip without disturbing neighboring cones.

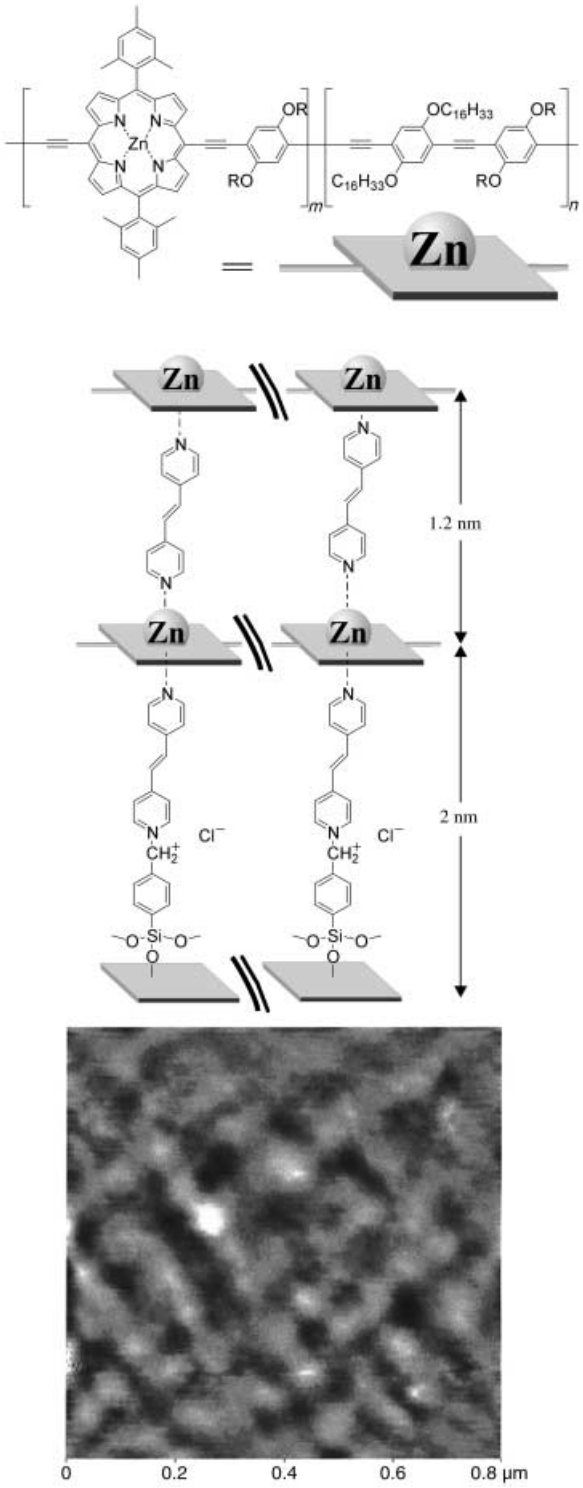

Figure 27. Model and AFM picture of the netlike, rigid zinc porphyrinate polymer, which is linked to multilayers by axial ligands.

7. Unmovable, Aqueous Molecules at Interfaces

Neither in ice nor in liquid water is the orientation of the water molecules such that hydrogen bonds connect only two specific oxygen atoms. Relocations of protons (i.e. nonlinear networks) frequently occur. In each case only one hydrogen atom lies on every oxygen–oxygen axis, but many configurations are possible and none are particularly preferred.[104, 105] Two borderline structures of ice define the possible configurations: 1) in the usual ice XI (or I_c) configuration the oxygen atoms form chairlike hexagonal rings similar to the diamond structure with the hydrogen atoms lying preferentially on the connecting lines between the oxygen atoms; 2) in the pentagonal ice arrangement, the oxygen atoms are positioned at the corners of planar pentagonal rings and assemble into dodecahedral $(H_2O)_{20}$ units. Such structures have been observed in gas hydrates[105, 106] (Figure 29). Between these two extremes lie many other hydrate structures, which consist of 5^n and 6^n polyhedra. The transformation from

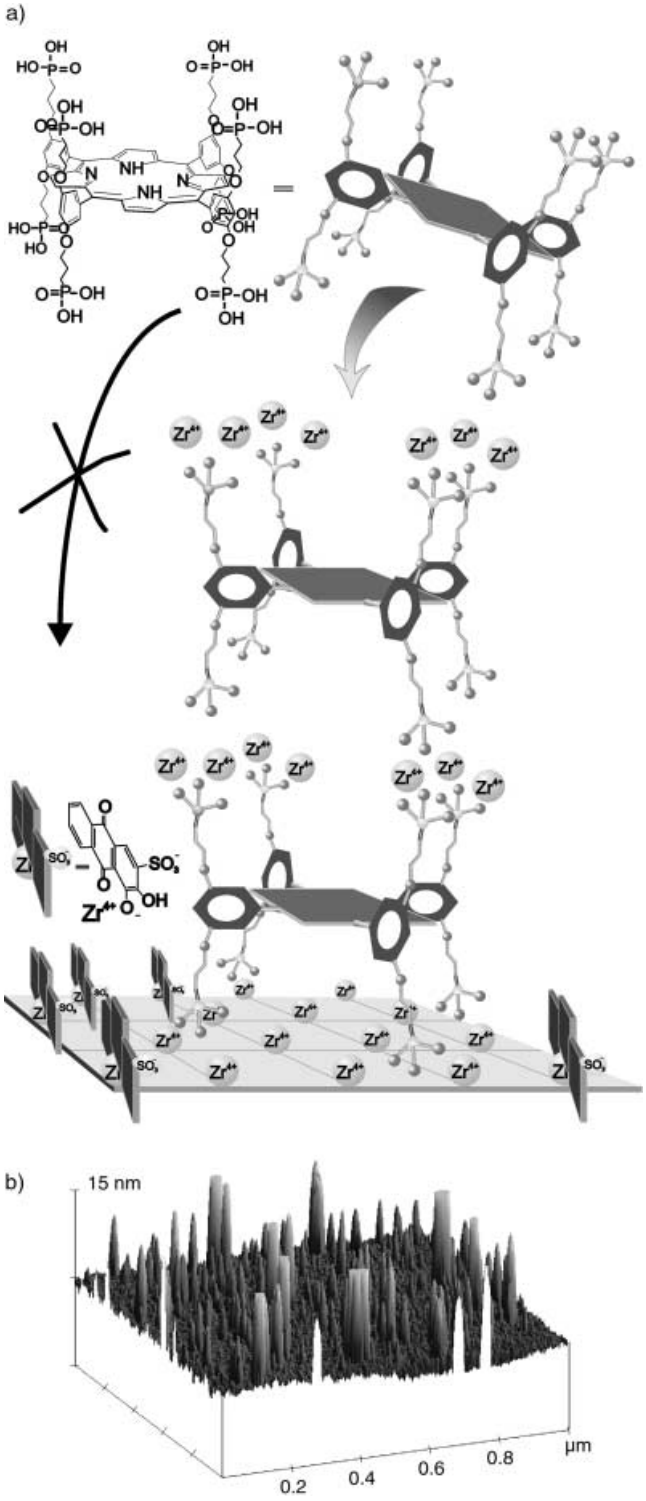

Figure 28. a) Model of the construction of pophyrin rocks on zirconium(IV)-covered silicon surfaces by stepwise self-assembly. Capping with Alizarin S restricts the number of conelike rocks. b) AFM picture of porphyrin cones on silicon (without capping).

amorphous ice to hexagonal ice is catalyzed by the incorporation of KOH (0.06 M). It seems to be effective, because it decreases the number of freely movable protons drastically. Single crystals of ice for neutron diffraction were thus obtained and allowed the localization of protons by neutron diffraction.[107]

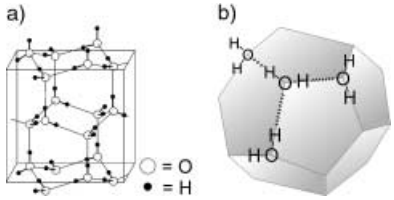

Figure 29. Crystal structures of a) hexagonal water in ice XI and b) of pentagonal water in clathrates and hydrophobic surfaces.

Water in hydrophobic clefts is immobile and can be used as a functional part of a landscape. It must, however, be stabilized by dissolved molecules (solutes), which are integrate into the water structure and aid the freezing process (Figure 30). Little is known about the kinetic inertness of thin aqueous films on hydrophobic surfaces in contact with bulk water. It has, for example, been demonstrated that motions within micrometer-thick layers of ice on metallic ruthenium at $-130\,^{\circ}C$ were much faster than the desorption of the molecules in the outer layer. Diffusion measurements of $H_2{}^{18}O$ bilayers, which were evaporated from $H_2{}^{16}O$ layers of ice lying underneath, showed that the desorption and lateral mobility of the uppermost layers of water were extremely slow (hours),[108a] whereas mixing with the $H_2{}^{16}O$ layer of ice underneath was much faster. It was also found that water layers became stable only when they consisted of at least three bilayers, at which point they can incorporate nonpolar gas molecules such as N_2.[108b]

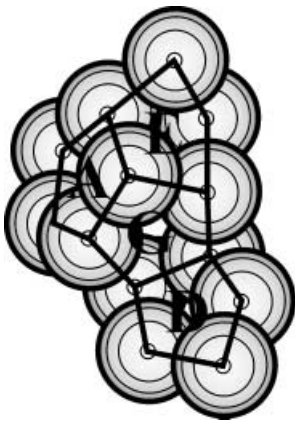

Figure 30. The water structure on the hydrophobic surface of the crambin protein. The concentric circles symbolize the height of the oxygen atoms (ring B is hidden).

Surface water on hydrophobic material mostly consists of the same clusters that can be found in liquid water or in the diamond-like orthorhombic ice XI (Figure 29a). At low temperatures ($<37\,^{\circ}C$) surface water is more ordered than bulk water. Surface ice, on the other hand, melts at low temperatures. However, in clathrate water (hydration water of crystalline inclusion compounds of hydrophobic organic compounds) pentagonal arrangements of water have been found as well as fullerene-like combinations of pentagonal and hexagonal rings.[105, 108] Furthermore, the interaction with hydrophobic surfaces compresses the structure of the water.[105, 106, 109]

Ordered hydrate coatings have been observed on hydrophobic surfaces of proteins. The highest resolution of the crystal structure of surface water was found for the protein crambin, in which a hydrophobic patch is covered by four water pentagons with a common peak (Figure 30, resolution 0.88 Å).[105, 110] In enzymes such water-binding areas function as active centers. In protease A of *S. griseus*, a water cluster is displaced from the protein, when it forms a complex with an

analogous substrate. Water clusters consisting of pentagons and occasionally of hexagons will only be well ordered if the protein offers anchor groups in suitable positions. In the case of crambin, the pentagons A and D are bound to the protein by hydrogen bonds, whereas B, C, and E are only bound by water–water interactions. A well ordered aqueous monolayer is thus formed on the hydrophobic surface; the monolayer consists of only 16 water molecules and is retained during crystallization. Such clathrate-analogous surface water could be bound equally tightly if the protein was surrounded by bulk water; an exchange of water molecules does not take place. Similar pentagonal structures have also been found on insulin, again on a hydrophobic protein surface around a hydrophilic tip.[105] In polar inorganic surroundings, the water decamer of ordinary ice seems to occur more frequently.[111]

Computer simulations of the water structure on planar walls showed that three or four molecular water layers formed a very stable ice-like structure.[109, 112] The water molecules next to the wall orientated their oxygen atoms towards the hydrophobic wall. However, these simulations did not disclose to what extent the ice-like water exchanges with the surrounding bulk water.

Charged molecules, which are anchored to the water surface by long alkyl chains, bind to counterions of appropriate size in bulk water about a thousand times stronger than the same molecules dissolved in bulk water. Hydrogen bonds formed in interfacial regions are also much stronger than those in the bulk water. This has been established, for example, for guanidinium-, calixarene-, and cyclic triazine diamine in ordered surface layers, which selectively bind to 10^{-4} M nucleotide and carbohydrate solutions in the water phase. The particular stability of the binding of the dissolved molecules to monolayers at the surface was related to a large decrease in the dielectric constant from 80 (water) to 2 (alkyl chains) at a distance of a few Ångströms. The quantum-mechanical reaction-field theory then shows a large enhancement of binding energy.[113]

Hydrophobic clefts with a width of 1–2 nm in lipid monolayers on smooth surfaces are filled with water when the electrodes are plunged into water. Neither hydrophobic repulsion nor formation of air bubbles occurs. Ferricyanide ions penetrate into the water-filled pores from the surrounding bulk water and produce simple CVs. The measured strength of the electric current through 0.6–2-nm membrane clefts does not change with rigid or fluid walls[64, 92, 114] (see Figure 24). Nonporous membranes show an almost perfect insulating effect.

The electron transport of ferricyanide ions through the water-filled membrane clefts was completely blocked when the electrode was first plunged for one hour into a 0.1M aqueous solution of 1,2-*trans*-cyclohexanediol, ascorbic acid, cellobiose, or tyrosine, then washed in water, and finally again plunged into the ferricyanide–KCl solution, which did not contain any organic solutes. The blocking effect lasted for several hours, in most cases even for months and ended only when HCl (pH 3)[114] or ethanol was added. Presumably the solutes formed three-dimensional hydrogen bond nets with surface water within the nanometer pores. HCl destroys the net by making the fluctuation of the protons easier (see crystallization in the presence of KOH; Figure 29a) and ethanol destroys the crystallinity of immovable water, because it can only build one hydrogen bond. CV investigations showed that dimethyl viologen worked as a "molecular stirring rod" and opened the pores.[115] Neither open-chained compounds, nor flexible cyclopentanediols, *cis*-1,2-cyclohexanediol or maltose had any blocking effect. It seems that the solutes fit into a pentagonal (ascorbic acid) or hexagonal (cellobiose) water structure thus strengthening it considerably. The model shown in Figure 31 suggests the formation of

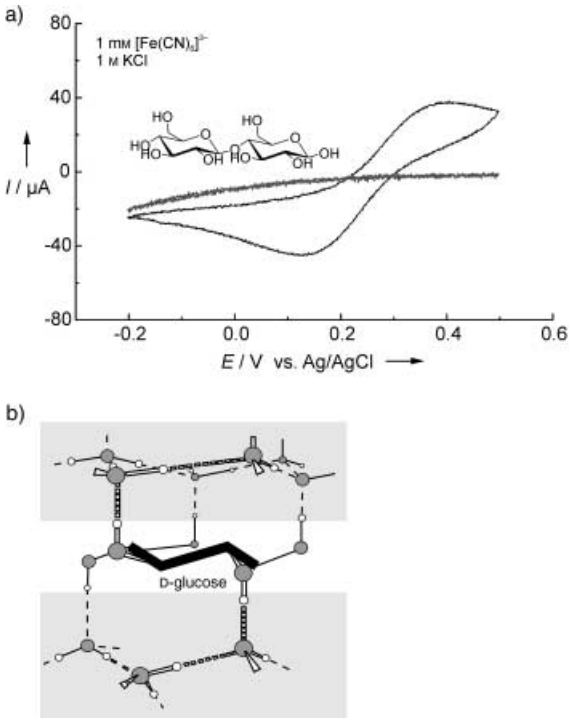

Figure 31. a) Cyclovoltammogram of ferricyanide at a porous octadecylsulfide membrane before (open curve) and after (closed curve) treatment with cellobiose, b) model of the ice plug with a glucose unit.

ice-like plugs induced by the rigid solute. The plugs are tightly connected to the hydrophobic walls of the membrane cleft. This tight structure does not allow diffusion of ferricyanide ions into the nanometer cleft and the slow electron transport from ions in bulk water by tunneling does not occur. The model does not explain the longevity of the "ice plug" positioned in direct contact with the bulk water. A dilution experiment provided a clue: the addition of 1% of maltose to the cellobiose totally eliminated its blocking effect. The entrapment of cellobiose in the cleft may thus be compared with that of a slow crystallization of already immobile surface water. Foreign molecules disturb this process.[115]

Similarly immovable water molecules have also been found in polar surroundings, that is, as large hydration spheres of potassium ions in layered thiophosphates. After replacing a bivalent cadmium ion by two hydrated potassium ions, the preformed layer system becomes associated in interlamellar regions in the form of monolayer water domains. On one side there was enough room for a unilateral hydration of

potassium ions, whereas the other side was occupied by hydrophobic sulfide ions of the thiophosphate grid. ^{1}H NMR Pake spectra of the pulverized thiophosphates showed movable and immovable water molecules side by side. The movable water could be removed in vacuum, whereas the immovable water could not (Figure 32). The position and splitting of the Pake doublets did not change with temperature. The exchange between the mobile and tightly-bound water molecules was at least 10^6 times slower than in bulk water. The rigid surrounding of the water monolayers clearly did not allow a widening of the hydrate cover and thus slowed down exchange reactions.[116]

Thin water layers on membrane surfaces serve as a medium for recognition processes between signal substances in surrounding bulk water and biological cell surfaces and hence further investigations are warranted.[117a–d] Cell-specific recognition processes between glycoproteins of differentiated cells and hormones can certainly not be attributed to high binding constants, which are unlikely in the case of carbohydrates in aqueous media, but rather to the kinetics of surface reactions. Water clusters that are immobilized and structurally defined by adequate carbohydrates may provide a perfect scenario for molecular trapping, for example, of a steroid hormone from the surface of its carrier protein in blood.

8. Colloidal Carrier Systems

The previously described membrane systems with form-stable clefts and hills can be characterized and then optimized on solid metal surfaces with the aid of fluorescence measurements, cyclic voltammetry, FTIR-spectroscopy, and scanning electron microscopy. The monolayers cannot be used on solid electrodes for NMR spectroscopic examinations of entrapped volumes of water, for photolysis experiments (charge separation and water splitting), and as catalysts in bulk water as the area (a few cm^2) of the large monolayers do not contain enough material ($\approx 10^{-10}-10^{-9}$ mol). The surface of membrane systems has to be enlarged and transferred into volume water to carry out flash photolysis experiments and solid-state NMR spectroscopy.

Spherical citrate gold particles (15–30 nm diameter; formed by the reduction of $AuCl_4^-$ with sodium citrate at 100) were found to be most suitable for experiments with closed membrane systems and form-stable nanometer clefts.[118–120] The smooth surface and curvature of citrate (citric acid gives rise to crystallites) largely corresponds to those of lipid vesicles. The curvature does not noticeably impair lateral interactions and the formation of closed lipid membranes. Smaller gold particles that contain many edges between crystal planes (e.g. Brust gold obtained from reduction with sodium borohydride)[121] do not allow the deposition of closed monolayers (Figure 33).

The use of citrate gold gives rise to some problems: 1) the particles are very heavy and sedimentation can occur during lengthy experiments; 2) the lipid membrane/gold mass ratio is very low ($\approx 1{:}10^3$); 3) the colloidal gold surfaces extinguish the fluorescence of directly applied dyes to a much greater extent than the rougher gold electrodes; 4) the flash photolysis of deposited dyes is difficult with strongly absorbing gold particles; 5) gold particles would be a prohibitively expensive system for the commercial production of hydrogen from water. Citrate gold is therefore only suitable for establishing synkinetic methods to produce well defined curved surfaces

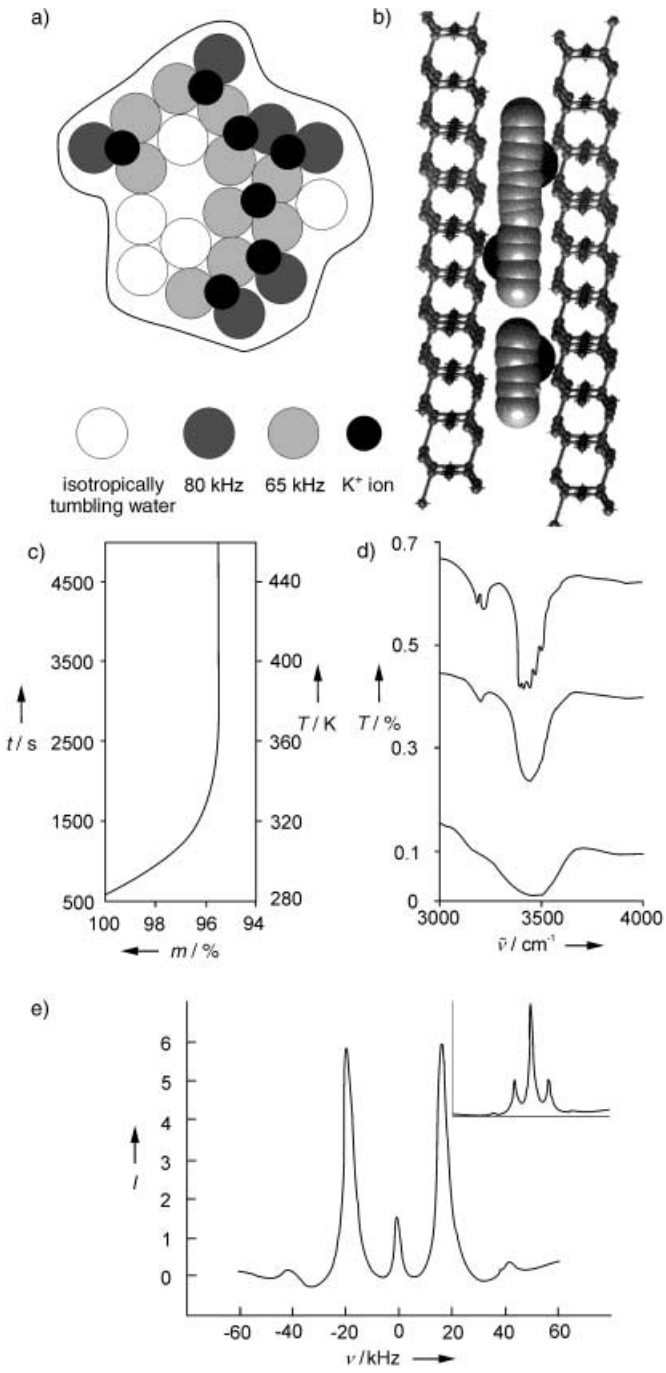

Figure 32. Trapped water in molecular cadmium–potassium thiophosphate layers. a, b) model of the three types of water between the crystal layers before (left) and after (right) vacuum drying. c) Isothermal weight loss in vacuo. d) IR spectra before (top), during (middle), and after (bottom) drying. e) PAKE ^{1}H NMR spectra before (insert) and after drying. The coupling constant of the remaining water (85 KHz) indicates immobile water molecules that surround the potassium ions; the isotropically movable water (a) produced doublets with a coupling constant of 65 KHz.

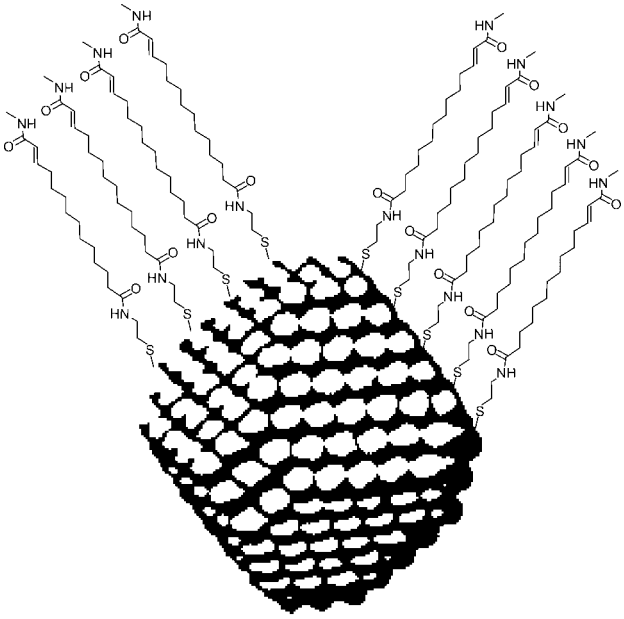

Figure 33. Typical disordered arrangement of membrane fragments on the crystal planes of 2–5-nm gold particles.

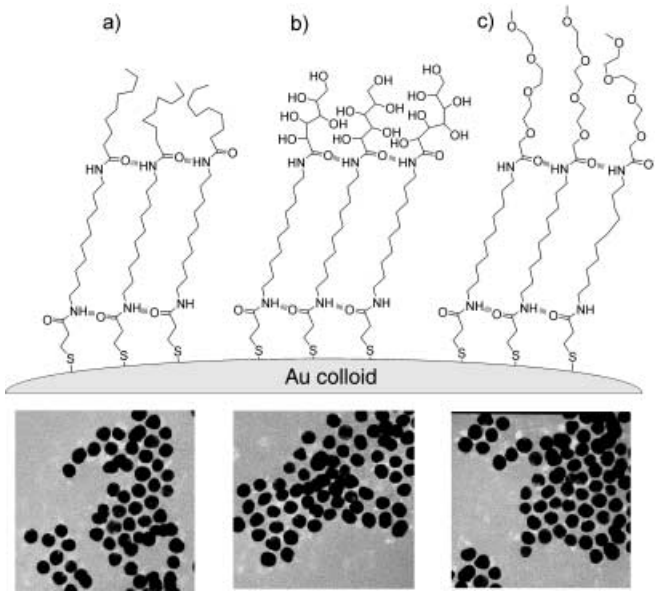

Figure 34. TEM pictures and models of solvatable gold colloids with a rigid, functional membrane core. a) soluble in toluene, b) soluble in water, c) soluble in toluene and water.

for characterization by electron microscopy and for electrochemical experiments. For photolytic processes such as the splitting of water, the reaction systems obtained have to be transferred to colloids, which do not absorb visible light.

The problem of sedimentation with 30 nm gold particles was solved by simple swelling and solvation of the outermost layer of the membrane coating. Introduction of a flexible 1–2 nm layer was sufficient. The inner part of the membranes is applied by self-assembly, can be rigid, and shows as many pores as are needed. The outer part can consist of loosely packed alkyl chains (for organic solvents) or open-chain gluconamide (for water). Oligoethylene glycol end groups stabilize the colloid in organic solvents as well as in water (Figure 34).[115]

The functional membrane/gold mass ratio can only be enhanced by flattening the spherical particles, not by shrinking them (see Figure 33). However, 5-nm thick gold platelets in aqueous solution would be a much better carrier system for solid-state NMR experiments. References to colloidal platelets can actually be found in earlier publications on "acetone gold".[118, 122] Own work along this line (reduction of gold chloride with citric acid and/or acetone in aqueous solution) produced thin crystalline platelets, which were characterized by TEM and a broad plasmon absorption (650 nm).

Reliable conservation of porphyrin fluorescence was more difficult. In the case of simple physical or chemical adsorption, at least 99% of the fluorescence of the porphyrins was quenched.[123] Roughening the surface of the gold, which had been helpful in the case of rigid gold electrodes, did not increase the fluorescence. Even when the chromophore was shielded from the gold surface by nonmetallic material, the problem of the plasmon absorption and fluorescence persisted.

Colloidal citrate gold was also bound to aminated indium/tin oxide (ITO) electrodes and then used as a basis for anchoring viologen catenanes. The viologen catenanes on the citrate film act as electron acceptors for tris(bipyridine)ruthenium in the excited state[123] and produce a photocurrent when irradiated with 434 nm light and with the support of a prepotential at the ITO-electrode. At 0.0 V all redox pairs produced a current and at < -0.6 V the viologen units were reduced and the photocurrent was blocked. A direct Ru* $\rightarrow$gold electron transport did not occur; the viologen transferred the electron to the metal. This corresponds to the classic Green–Shilov system in which a chemically reduced molecule reacts with platinum colloids and releases molecular hydrogen.[124, 125] The quantum yield of photoelectron formation was very low (10^{-4}); that of the Ru* $\rightarrow$Bipy electron transfer amounted to 5%.

Gold and silver particles in aqueous media were also dimerized by means of phenyl acetylene bridges of variable length. Dimers of 30-nm silver particles connected by short bridges showed the splitting and displacements of plasmon absorption bands typical for the electronic coupling of both particles[126] (Figure 35). Electron donor–acceptor systems with very large surface areas for charge separation may become accessible from such membrane-covered heterodimers.

Citrate gold was also entrapped in the form of linear chains within the pores of aluminum oxide membranes. Pyrrole polymerization within these pores produced a connective mantle. Afterwards the aluminum oxide was dissolved with KOH, and a one-dimensional chain of gold particles linked to polypyrrole was obtained. Since the polypyrrole has conductive properties, "electron hopping" between the gold clusters should be possible, similar to that observed in radical-containing acetylene or DNA polymers.[127] The rigidity of the pyrrole polymers allowed AFM manipulations of this system (Figure 36). Complementary DNA branches were also used successfully to interlink membrane-covered gold colloid

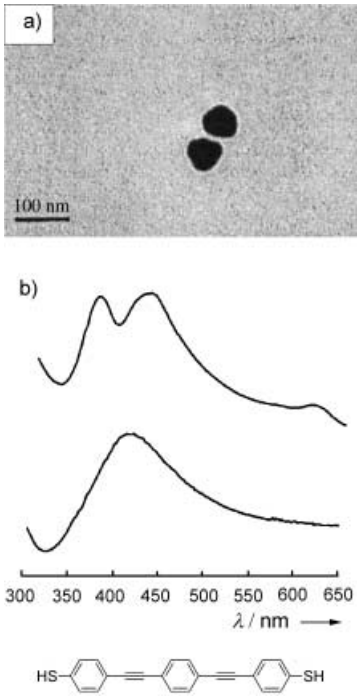

Figure 35. a) SEM pictures of a silver–colloid dimer bound by a rigid α,ω-disulfide. The distance is $\approx$20 nm. b) Plasmon spectrum of the monomeric silver colloid (bottom) and of the dimer (top).

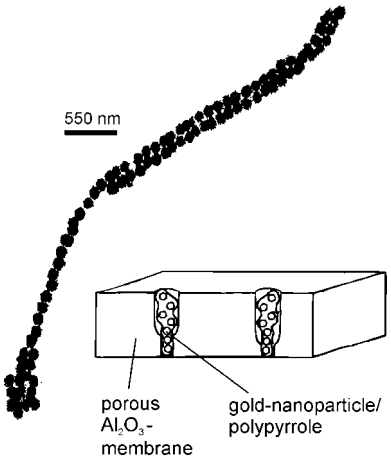

Figure 36. TEM picture of linear gold colloid wires with polypyrrole connections, which can be released from aluminum oxide pores.

particles, which melted sharply as is typical for DNA duplexes.[128]

ITO electrodes that are coated with a cationic 3-aminopropylsiloxane layer and are thus positively charged connect citrate gold particles as a porous monolayer. This layer absorbed at 520 nm and at 650 nm when packed more closely which corresponds to the absorption of gold foils. The same band shifting occurred when spherical gold particles were converted into platelets by treatment of citrate gold with acetone as mentioned above. Negatively charged citrate gold particles were also connected to a zinc porphyrinate through a spacer. Viologen was used as an anchor and electron acceptor. Upon irradiation with visible light, the energy-rich electrons of the porphyrin were transferred to the electrode and a

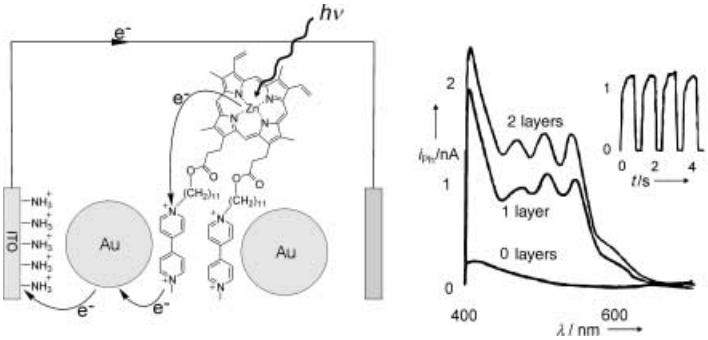

Figure 37. Positive charges of viologen substituents on porphyrin molecules connect gold colloids and gold electrodes. A layer consists of a combination of a citrate gold layer with a layer of porphyrin counterions (the left picture shows 1.5 layers). When the system is irradiated in the presence of weak reductants, photoelectric currents flow after about one second. The wave dependence of this photoelectric current corresponds to the absorption spectrum of the porphyrin.

photoelectric current of several nanoampere was measured (Figure 37).[129]

Spherical gold particles are also soft enough to penetrate into clefts on the surface of globular proteins. It has for example been found that cytochrome with naked ITO electrodes did not produce any electric contact, but did so when gold colloids were deposited between the proteins and the electrode. Many electrochemical chain reaction can thus be established by combining gold-colloids with proteins.[130] Furthermore, 4–5 nm gold particles that are only partly covered by octadecanethiol move together so closely by interdigitation of the incomplete monolayer surface that 2-nm long aryldithiols connect the gold particles and allow a current to flow. Monolayers of colloids then also conduct currents when anchored to a nonconducting substrate.

Mesoscopic polyelectrolyte films with alternating charges compete with the rigid monolayers described herein. They are also accessible by applying dip and wash procedures and can also be loaded with cationic and anionic dyes.[131, 132]

9. Summary and Outlook

Rigid molecular assemblies in bulk water and in landscapes on support systems allow complex arrangements of reactive components. This Review described domains, micelles, vesicles, and fibers in bulk water as well as in the dry state, followed by monolayers on gold, immobile volumes of water in membrane clefts on solid surfaces, and finally rigid lipid membranes on gold colloids in solution. This sequence is only logical under the aspect of systematically building up chain reactions by means of synkinesis.

The structures of the systems produced so far have been visualized be means of AFM, STM, and TEM, and were characterized indirectly by fluorescence quenching and cyclic voltammetry. The determination of the changes in molecular conformation by solid-state ^{13}C NMR spectroscopy in the transition from 3D crystals to noncovalent fibers was only possible with glyconamide. This structural analysis was successful because the fibers were isolated in the solid state

in gram quantities and because their solid-state NMR spectra could be correlated with those of many 3D crystals whose structure had already been determined by X-ray crystallographic analysis. Molecular structures on solid supports, in particular at membrane edges and in immobile water volumes, and the utilization of the chemical reactivity of the components (catalysis, light-induced charge separation) has been investigated indirectly only on gold electrodes. Colloids present new problems: Appropriately-sized gold colloids absorb light and are therefore not suitable for flash photolysis experiments. Silicates, on the other hand, tend to produce pores with a high curvature and with different depths which renders the construction of closed membranes and clefts virtually impossible. Poreless CaBosil particles were unstable in self-assembly processes: they tended to swell and to formed threads. Semiconductor colloids are notoriously sensitive to oxygen, acids, and bases and little is known about the stability of smooth surfaces. What matters in synkineses is the production of colloid particles whose surfaces remain both reactive and smooth in several self-assembly steps and which do not disturb photochemical and electrochemical experiments.

The Review answers the frequently asked question: why is the term "synkinesis"[2] necessary in supramolecular chemistry? Why do the terms self-assembly and supramolecular synthesis not suffice? There is no "self" in complex systems (e.g., see Figures 25, 26 and 29) as every single component of molecular systems has to be optimized with regard to size, charge, counterion, solubility, adhesion to surfaces, redox potential, fluorescence, etc. The synkinetic chemist combines molecules that fit with each other. The synthesis of these synkinons need careful plans. New syntheses will be necessary if anything does not fit or stick tightly to the system. Finally, if the required system has been obtained in quantitative yields (systems cannot be cleaned!), it would be the result of planning, successful experiments, and optimization. Synkinesis is consequently analogous to a successful synthesis. After all, a Grignard reaction is not a "self-assembly" simply because negatively and positively charged carbon atoms reacted together "by themselves".

A cursory comparison of the figures in books on self-assembly[1, 68, 133] and synkinesis[2] reveals the difference between physical and organic chemistry of the membrane. Structural formula, stereochemistry, optimized yields in multistage synkinesis, and complex synkinons are only made in laboratories active in organic chemistry. Physical chemists describe molecules and their fragments as spheres, cones, cylinders, and wavy lines that are assembled according to the laws of elementary geometry and thermodynamics. In this respect it is justified, but not very helpful as a basis for the construction of complex systems.

Synkinesis is the creation of well defined and isolable molecular assemblies in the same rational way that cyclic, helical, branched, rigid, or flexible polymers are synthesized. In this case too one speaks of synthesis and not of self-assembly. The term synkinesis refers directly to a multistage process in which all reactions are completely reversible. In many cases, heating or changing the pH value is sufficient for a complete dissolution into monomers or a reconstitution of high-molecular-weight systems. The term "supramolecular synthesis" would also be applicable, but is no longer appropriate as most "supramolecular" molecules currently produced consist of interlocked rings or of several molecular subunits connected by covalent bonds.

What can be expected of rigid mono- and bilayers and of molecular landscapes? The application of fluid membranes to organize chain reaction mostly fails because the components are too flexible and neither distances nor orientations can be fixed. Rigid and reactive membrane systems on nanoparticles hopefully behave more like biosystems anchored by membrane proteins. A 1-cm^2 area of a gold electrode or of a silicon microchip may carry 10^{10} separate landscape motifs, which can all be oxidized, reduced, shifted, eroded, enlarged, and coated separately and offer an almost infinite number of possibilities for manipulation. In restricted areas it should be possible to interconnect valleys, hills in vectorial chain reactions.

Financial support by the Deutsche Forschungsgemeinschaft (SFB 312 "Vectorial Membrane Processes" and SFB 448 "Mesoscopic Systems"), the European TMR-networks "Artificial Photosynthesis" and "Carbohydrate Recognition", by the Fonds der Deutschen Chemischen Industrie, and by the Förderkomission der Freien Universität Berlin is gratefully acknowledged. We thank Dr. Laurent Ruhlmann and Dr. Jörg Zimmermann for their major contributions to the characterization of nanometer pores. Dr. Marie-Françoise Gouzy developed the kanamycin micelles. Dr. Christoph Böttcher and Dr. Christian Messerschmidt worked as pioneers in AFM, STM, and TEM of molecular landscapes. We also thank the referees of our manuscript for their helpful and constructive reviews.

Received: May 7, 2001 [A 472]

[1] J. N. Israelachvili, *Intermolecular and Surface Forces*, Academic Press, London, **1985**.
[2] a) J.-H. Fuhrhop, J. Köning in *Monographs in Supramolecular Chemistry; Molecular Assemblies and Membranes: The Synkinetic Approach* (Ed.: J. F. Stoddart), Royal Society of Chemistry, London, **1994**, pp. i-xiii; b) J. H. Fuhrhop, C. Endisch, *Molecular and Supramolecular Chemistry of Natural Products and Model Compounds*, Marcel Dekker, New York, **2000**.
[3] a) J.-H. Fuhrhop, *Angew. Chem.* **1974**, *86*, 363; *Angew. Chem. Int. Ed. Engl.* **1974**, *13*, 321; b) J.-H. Fuhrhop, *Angew. Chem.* **1976**, *88*, 704; *Angew. Chem. Int. Ed. Engl.* **1976**, *15*, 648; c) J.-H. Fuhrhop, J. Mathieu, *Angew. Chem.* **1984**, *96*, 124; *Angew. Chem. Int. Ed. Engl.* **1984**, *23*, 100.
[4] F. M. Menger, *Acc. Chem. Res.* **1979**, *12*, 111.
[5] J. S. Nowick, J. S. Chen, G. Noronha, *J. Am. Chem. Soc.* **1993**, *115*, 7636.
[6] R. P. Bonar-Law, *J. Org. Chem*. **1996**, *61*, 3623.
[7] P. Juvvadi, S. Vunnam, R. B. Merrifield, *J. Am. Chem. Soc*. **1996**, *118*, 8989.
[8] N. Sakai, D. Gerard, S. Matile, *J. Am. Chem. Soc.* **2001**, *123*, 2517.
[9] O. S. Andersen, *J. Phys. Chem*. **2001**, *100*, 4622.
[10] R. R. Ketchem, W. Hu, T. A. Cross, *Science* **1993**, *261*, 1457.
[11] O. S. Andersen, R. E. Koeppe II, *Physiol. Rev.* **1992**, *72*, 89.
[12] B. A. Cornell, V. L. B. Braach-Maskvytis, L. G. King, P. D. J. Osman, B. Raguse, L. Wieczorek, R. J. Pace, *Nature* **1997**, *387*, 580.
[13] J.-H. Fuhrhop, M. Krull, A. Schulz, D. Möbius, *Langmuir* **1990**, *6*, 497.

[14] J.-H. Fuhrhop, U. Liman, V. Koesling, *J. Am. Chem. Soc.* **1988**, *110*, 6840.
[15] J. D. Hartgerink, J. R. Granja, R. A. Milligan, M. R. Ghadiri, *J. Am. Chem. Soc.* **1996**, *118*, 43.
[16] H. S. Kim, J. D. Hartgerink, M. R. Ghadiri, *J. Am. Chem. Soc.* **1998**, *120*, 4417.
[17] K. Motesharei, R. Ghadiri, *J. Am. Chem. Soc.* **1997**, *119*, 11312.
[18] T. D. Clark, L. K. Buehler, M. R. Ghadiri, *J. Am. Chem. Soc.* **1998**, *120*, 651.
[19] T. S. Arrhenius, M. Blanchard-Desce, M. Dvolaitzky, J.-M. Lehn, J. Malthete, *Proc. Natl. Acad. Sci. USA* **1986**, *83*, 5355.
[20] a) G. W. Gokel, O. Murillo, *Acc. Chem. Res.* **1996**, *29*, 425; b) L. A. Weiss, N. Sakai, B. Ghebremariam, C. Ni, S. Matile, *J. Am. Chem. Soc.* **1997**, *119*, 12142.
[21] a) G. Leatherman, E. N. Durantini, D. Gust, T. A. Moore, S. Stone, Z. Zhou, P. Rez, Y. Z. Liu, S. M. Lindsay, *J. Phys. Chem. B* **1999**, *103*, 4006; b) S. Creager, C. J. Yu, C. Bamdad, S. O'Connor, T. MacLean, E. Lam, Y. Chong, G. T. Olsen, J. Luo, M. Gozin, J. F. Kayyem, *J. Am. Chem. Soc.* **1999**, *121*, 1059.
[22] a) V. Subramanian, W. A. Ducker, *Langmuir* **2000**, *16*, 4447; b) V. Subramanian, W. A. Ducker, *J. Phys. Chem. B* **2001**, *105*, 1389.
[23] M. Gouzy, F. Gonzaga, M. Lauer, A. Schulz, C. Boettcher, J.-H. Fuhrhop, *Langmuir*, submitted.
[24] C. Draeger, C. Boettcher, C. Messerschmidt, L. Ruhlmann, J.-H. Fuhrhop, U. Siggel, L. Hammerström, *Langmuir* **2000**, *16*, 2068.
[25] B. Klarewicz, C. Draeger, K. Jansen, J.-H. Fuhrhop, unpublished results.
[26] C. Messerschmidt, C. Draeger, A. Schulz, J. P. Rabe, J.-H. Fuhrhop, *Langmuir* **2001**, *17*, 3526.
[27] M. F. Roks, H. G. J. Visser, J. W. Zwikker, A. J. Verkley, R. J. M. Nolte, *J. Am. Chem. Soc.* **1983**, *105*, 4507.
[28] H. Ohno, S. Takeoka, E. Tsuchida, *Polymer Bull.* **1985**, *14*, 487.
[29] H. Ringsdorf, B. Schlarb, J. Venzmer, *Angew. Chem.* **1988**, *100*, 117; *Angew. Chem. Int. Ed. Engl.* **1988**, *27*, 113.
[30] L. Zhang, A. Eisenberg, *J. Am. Chem. Soc.* **1996**, *118*, 3168.
[31] a) S. Klingelhöfer, W. Heitz, A. Greiner, S. Oestreich, S. K. Förster, M. Antonietti, *J. Am. Chem. Soc.* **1997**, *119*, 10116; b) M. Schreuder Goedheijt, B. E. Hanson, J. N. H. Reek, P. C. J. Kramer, P. W. N. M. van Leeuwen, *J. Am. Chem. Soc.* **2000**, *122*, 1650.
[32] a) S. A. Jenekhe, X. L. Chen, *Science* **1998**, *279*, 1903; b) B. M. Discher, Y. Y. Won, D. S. Ege, J. C. M. Lee, F. S. Bates, D. E. Discher, D. A. Hammer, *Science* **1999**, *284*, 1143.
[33] G. T. Oostergetel, F. J. Esselink, G. Hadziioannou, *Langmuir* **1995**, *11*, 3721.
[34] N. H. Thomson, I. Collin, M. C. Davies, K. Palin, D. Parkins, C. J. Roberts, S. J. B. Tendler, P. M. Williams, *Langmuir* **2000**, *16*, 4813.
[35] T. Komatsu, E. Tsuchida, C. Boettcher, D. Donner, C. Messerschmidt, U. Siggel, W. Stocker, J. P. Rabe, J.-H. Fuhrhop, *J. Am. Chem. Soc.* **1997**, *119*, 11660.
[36] J.-H. Fuhrhop, W. Helfrich, *Chem. Rev.* **1993**, *93*, 1565.
[37] J. H. Fuhrhop, P. Schnieder, J. Rosenberg, E. Boekema, *J. Am. Chem. Soc.* **1987**, *109*, 3387.
[38] J. Köning, C. Boettcher, H. Winkler, E. Zeitler, Y. Talmon, J.-H. Fuhrhop, *J. Am. Chem. Soc.* **1993**, *115*, 693.
[39] J.-H. Fuhrhop, C. Boettcher, *J. Am. Chem. Soc* **1990**, *112*, 1768.
[40] T. Kunitake, Y. Okahata, M. Shimomura, S. Yasunami, K. Takarabe, *J. Am. Chem. Soc.* **1985**, *107*, 509.
[41] J.-H. Fuhrhop, C. Demoulin, J. Rosenberg, C. Boettcher, *J. Am. Chem. Soc.* **1990**, *112*, 2827.
[42] T. Tachibana, T. Yoshizumi, K. Hori, *Bull. Chem. Soc. Jpn.* **1979**, *52*, 34.
[43] J.-H. Fuhrhop, T. Bedurke, A. Hahn, S. Grund, J. Gatzmann, M. Riederer, *Angew. Chem.* **1994**, *106*, 351; *Angew. Chem. Int. Ed. Engl.* **1994**, *33*, 350.
[44] J.-H. Fuhrhop, M. Krull, G. Büldt, *Angew. Chem.* **1987**, *99*, 707; *Angew. Chem. Int. Ed. Engl.* **1987**, *26*, 699.
[45] S. Svenson, B. Kirste, J.-H. Fuhrhop, *J. Am. Chem. Soc.* **1994**, *116*, 11969.
[46] I. Sack, S. Macholl, J.-H. Fuhrhop, G. Buntkowsky, *Phys. Chem. Chem. Phys.* **2000**, *2*, 1781.
[47] C. Messerschmidt, S. Svenson, W. Stocker, J.-H. Fuhrhop, *Langmuir* **2000**, *16*, 7445.
[48] J.-H. Fuhrhop, D. Spiroski, C. Boettcher, *J. Am. Chem. Soc.* **1993**, *115*, 1600.
[49] J.-H. Fuhrhop, P. Blumtritt, C. Lehmann, P. Luger, *J. Am. Chem. Soc.* **1991**, *113*, 7437.
[50] C. Messerschmidt, A. Schulz, J. Zimmermann, J.-H. Fuhrhop, *Langmuir* **2000**, *16*, 5790.
[51] I. Inamura, K. Uchida, *Bull. Chem. Soc. Jpn.* **1991**, *64*, 2005.
[52] a) J.-H. Fuhrhop, C. Demoulin, C. Boettcher, J. Köning, U. Siggel, *J. Am. Chem. Soc.* **1992**, *114*, 4159; b) J.-H. Fuhrhop, U. Bindig, U. Siggel, *J. Chem. Soc. Chem. Commun.* **1994**, 1583.
[53] B. Rosengarten, C. Böttcher, A. Schulz, J.-H. Fuhrhop, U. Siggel, *J. Porphyrins Phthalocyanines* **1998**, *2*, 273.
[54] J.-H. Fuhrhop, U. Bindig, U. Siggel, *J. Am. Chem. Soc.* **1993**, *115*, 11036.
[55] C. Endisch, C. Böttcher, J.-H. Fuhrhop, *J. Am. Chem. Soc.* **1995**, *117*, 8273.
[56] D. Donner, C. Böttcher, C. Messerschmidt, U. Siggel, J.-H. Fuhrhop, *Langmuir* **1999**, *15*, 5029.
[57] H. von Berlepsch, C. Böttcher, A. Quart, M. Regenbrecht, S. Akari, U. Keiderling, H. Schnablegger, S. Dähne, S. Kirstein, *Langmuir* **2000**, *16*, 5908.
[58] G. Scheibe, *Angew. Chem.* **1936**, *49*, 563; G. Scheibe, *Angew. Chem.* **1937**, *50*, 51.
[59] E. E. Jelley, *Nature* **1936**, *138*, 1009; E. E. Jelley, *Nature* **1937**, *139*, 631.
[60] S. Daehne, *Photogr. Sci. Eng.* **1979**, *23*, 219.
[61] V. Czikklely, H. D. Försterling, H. Kuhn, *Chem. Phys. Lett.* **1970**, *6*, 207.
[62] M. T. Cygan, G. E. Collins, T. D. Dunbar, D. L. Allara, C. G. Gibbs, C. D. Gutsche, *Anal. Chem.* **1999**, *71*, 142.
[63] N. J. Tao, Z. Shi, *J. Phys. Chem.* **1994**, *98*, 1464.
[64] W. Fudickar, J. Zimmermann, L. Ruhlmann, B. Roeder, U. Siggel, J.-H. Fuhrhop, *J. Am. Chem. Soc.* **1999**, *121*, 9539.
[65] X. Qiu, C. Wang, Q. Zeng, B. Xu, S. Yin, H. Wang, *J. Am. Chem. Soc.* **2000**, *122*, 5550.
[66] J.-H. Fuhrhop, T. Bedurke, M. Gnade, J. Schneider, K. Doblhofer, *Langmuir* **1997**, *13*, 455.
[67] Z. P. Yang, I. Engquist, J.-M. Kauffmann, B. Liedberg, *Langmuir* **1996**, *12*, 1704.
[68] A. Ulman, *Ultrathin Organic Films*, Academic Press, New York, **1991**.
[69] J. Sagiv, *J. Am. Chem. Soc.* **1980**, *102*, 92.
[70] J. Sagiv, *Isr. J. Chem.* **1979**, *18*, 346.
[71] R. Maoz, H. Cohen, J. Sagiv, *Langmuir* **1998**, *14*, 5988.
[72] D. N. Batchelder, S. D. Evans, T. L. Freeman, L. Häussling, H. Ringsdorf, H. Wolf, *J. Am. Chem. Soc.* **1994**, *116*, 1050.
[73] S. D. Evans, K. E. Goppert-Berarducci, E. Urankar, L. J. Gerenser, A. Ulman, *Langmuir* **1991**, *7*, 2700.
[74] A. J. Black, T. T. Wooster, W. E. Geiger, M. N. Paddon-Row, *J. Am. Chem. Soc.* **1993**, *115*, 7924.
[75] W. S. V. Kwan, L. Atanaoska, L. L. Miller, *Langmuir* **1991**, *7*, 1419.
[76] W. S. V. Kwan, V. Cammarate, L. L. Miller, M. G. Hill, K. R. Mann, *Langmuir* **1992**, *8*, 3003.
[77] Y. S. Obeng, M. E. Laing, A. C. Friedli, H. C. Yang, D. Wang, E. W. Thulstrup, A. J. Bard, J. Michl, *J. Am. Chem. Soc.* **1992**, *114*, 9943.
[78] S.-W. Tam-Chang, H. A. Biebuyck, G. M. Whitesides, N. Jeon, R. G. Nuzzo, *Langmuir* **1995**, *11*, 4371.
[79] R. S. Clegg, J. E. Hutchison, *Langmuir* **1996**, *12*, 5239.
[80] P. Böhme, H.-G. Hicke, C. Böttcher, J.-H. Fuhrhop, *J. Am. Chem. Soc.* **1995**, *117*, 5824.
[81] R. S. Clegg, S. M. Reed, R. K. Smith, B. L. Barron, J. A. Rear, J. E. Hutchison, *Langmuir* **1999**, *15*, 8876.
[82] M.-W. Tsao, C. L. Hoffmann, J. F. Rabolt, H. E. Johnson, D. G. Castner, C. Erdelen, H. Ringsdorf, *Langmuir* **1997**, *13*, 4317.
[83] T. J. Lenk, V. M. Hallmark, C. L. Hoffmann, J. F. Rabolt, *Langmuir* **1994**, *10*, 4610.
[84] J. Schneider, C. Messerschmidt, A. Schulz, M. Gnade, B. Schade, P. Luger, P. Bombicz, V. Hubert, J.-H. Fuhrhop, *Langmuir* **2000**, *16*, 8575.
[85] O. Chailapakul, R. M. Crooks, *Langmuir* **1993**, *9*, 884.

[86] V. Chechik, R. M. Crooks, C. J. M. Stirling, *Adv. Mater.* **2000**, *12*, 1161.
[87] E. Sabatani, J. Cohen-Boulakia, M. Bruening, I. Rubinstein, *Langmuir* **1993**, *9*, 2974.
[88] J. F. Kang, A. Ulman, S. Liao, R. Jordan, *Langmuir* **1999**, *15*, 2095.
[89] J. F. Kang, A. Ulman, S. Liao, R. Jordan, G. Yand, G.-Y. Liu, *Langmuir* **2001**, *17*, 95.
[90] R. W. Zehner, L. R. Sita, *Langmuir* **1997**, *13*, 2973.
[91] M. T. Cygan, T. D. Dunbar, J. J. Arnold, L. A. Bumm, N. F. Shedlock, T. P. Burgin, L. Jones II, D. L. Allara, J. M. Tour, P. S. Weis, *J. Am. Chem. Soc.* **1998**, *120*, 2721.
[92] M. Skupin, G. Li, W. Fudickar, J. Zimmermann, B. Röder, J.-H. Fuhrhop, *J. Am. Chem. Soc.* **2001**, *123*, 3454.
[93] Y. Xia, G. M. Whitesides, *Angew. Chem.* **1998**, *110*, 568; *Angew. Chem. Int. Ed.* **1998**, *37*, 550.
[94] M. Geissler, A. Bernard, A. Bietsch, H. Schmidt, B. Michel, E. Delamarche, *J. Am. Chem. Soc.* **2000**, *122*, 6303.
[95] C. Messerschmidt, A. Schulz, J. P. Rabe, A. Simon, J.-H. Fuhrhop, *Langmuir* **2000**, *16*, 1299.
[96] K. Araki, M. J. Wagner, M. S. Wrighton, *Langmuir* **1996**, *12*, 5393.
[97] D. A. Offord, S. B. Sachs, M. S. Ennis, T. A. Eberspacher, J. H. Griffin, C. E. D. Chidsey, J. P. Collman, *J. Am. Chem. Soc.* **1998**, *120*, 4478.
[98] D. M. Sarno, B. Jiang, D. Grosfeld, J. O. Afriyie, L. J. Matienzo, W. E. Jones, Jr., *Langmuir* **2000**, *16*, 6191.
[99] M. S. Boeckl, A. L. Bramblett, K. D. Hauch, T. Sasaki, B. D. Ratner, J. W. Rogers, Jr., *Langmuir* **2000**, *16*, 5644.
[100] A. Alberti in *Comprehensive Supramolecular Chemistry*, *Vol. 7* (Ed.: J.-M. Lehn), Pergamon, Oxford, **1996**, p. 151.
[101] M. Fang, D. M. Kaschak, A. C. Sutorik, T. E. Mallouk, *J. Am. Chem. Soc.* **1997**, *119*, 12184.
[102] A. Klyszcz, M. Lauer, J.-H. Fuhrhop, unpublished results.
[103] A. Neuhaus, *Fortschr. Mineral.* **1950/51**, *29/30*, 138.
[104] L. Pauling, *J. Am. Chem. Soc.* **1935**, *57*, 2680.
[105] G. A. Jeffrey, W. Saenger, *Hydrogen Bonding in Biological Structures*, Springer, Heidelberg, **1991**, p. 425.
[106] P. T. Beurskens, G. A. Jeffrey, *J. Chem. Phys.* **1964**, *40*, 2800.
[107] S. M. Jackson, V. M. Nield, R. W. Whitworth, M. Oguro, C. C. Wilson, *J. Phys. Chem. B* **1997**, *101*, 6142.
[108] a) D. E. Brown, S. M. George, *J. Phys. Chem.* **1996**, *100*, 15460; b) Y. Lilach, L. Romm, T. Livnch, M. Asscher, *J. Phys. Chem. B* **2001**, *105*, 2736.
[109] K. A. T. Silverstein, A. D. J. Haymet, K. A. Dill, *J. Am. Chem. Soc.* **1998**, *120*, 3166.
[110] M. M. Teeter, S. M. Roe, N. H. Heo, *J. Mol. Biol.* **1993**, *230*, 292.
[111] L. J. Barbour, G. W. Orr, J. L. Atwood, *Nature* **1998**, *393*, 671.
[112] M. Vossen, F. Forstmann, *J. Chem. Phys.* **1994**, *101*, 2379.
[113] K. Ariga, T. Kunitake, *Acc. Chem. Res.* **1998**, *31*, 371.
[114] J.-H. Fuhrhop, T. Bedurke, M. Gnade, J. Schneider, K. Doblhofer, *Langmuir* **1997**, *13*, 455.
[115] G. Li, J.-H. Fuhrhop, *Angew. Chem.*, in press.
[116] N. Arun, S. Vasudevan, K. V. Ramanathan, *J. Am. Chem. Soc.* **2000**, *122*, 6028.
[117] a) H. S. Frank, W. M. Evans, *J. Chem. Phys.* **1945**, *13*, 507; b) J. Israelachvili, H. Wennerstroem, *Nature* **1996**, *379*, 219; c) R. U. Lemieux, *Acc. Chem. Res.* **1996**, *29*, 373; d) B. Kirchner, D. J. Searles, A. J. Dyson, P. S. Vogt, H. Huber, *J. Am. Chem. Soc.* **2000**, *122*, 5379.
[118] J. Turkevich, P. C. Stevenson, J. Hillier, *Faraday Discuss.* **1951**, *11*, 55.
[119] S. Biggs, P. Mulvaney, C. F. Zukoski, F. Grieser, *J. Am. Chem. Soc.* **1994**, *116*, 9150.
[120] K. C. Grabar, R. G. Freeman, M. B. Hommer, M. J. Natan, *Anal. Chem.* **1995**, *67*, 735.
[121] A. C. Templeton, W. P. Wuelfing, R. W. Murray, *Acc. Chem. Res.* **2000**, *33*, 27.
[122] J. Davies, *J. Phys. Chem.* **1929**, *33*, 276.
[123] M. Lahav, V. Heleg-Shabtai, J. Wasserman, E. Katz, I. Willner, H. Dürr, Y.-Z. Hu, S. H. Bossmann, *J. Am. Chem. Soc.* **2000**, *122*, 11480.
[124] D. E. Green, L. H. Stickland, *Biochem. J.* **1934**, *28*, 898.
[125] B. V. Koryakin, T. S. Dzhabier, A. E. Shilov, *Dokl. Akad. Nauk SSSR* **1977**, *233*, 620.
[126] W. P. McConnell, J. P. Novak, L. C. Brousseau III, R. R. Fuierer, R. C. Tenent, D. L. Feldheim, *J. Phys. Chem. B* **2000**, *104*, 8925.
[127] S. M. Marinakos, D. A. Shultz, D. L. Feldheim, *Adv. Mater.* **1999**, *11*, 34.
[128] C. A. Mirkin, R. L. Letsinger, R. C. Mucic, J. J. Storkoff, *Nature* **1996**, *382*, 607.
[129] A. N. Shipway, M. Lahav, I. Willner, *Adv. Mater.* **2000**, *12*, 993.
[130] a) K. R. Brown, A. P. Fox, M. J. Natan, *J. Am. Chem. Soc.* **1996**, *118*, 1154; b) K. C. Grabar, K. J. Allison, B. E. Baker, R. M. Bright, K. R. Brown, R. G. Freeman, A. P. Fox, C. D. Keating, M. D. Musick, M. J. Natan, *Langmuir* **1996**, *12*, 2353; c) A. Gole, C. Dash, V. Ramakrishnan, S. R. Sainkar, A. B. Mandale, M. Rao, M. Sastry, *Langmuir* **2001**, *17*, 1674.
[131] G. Decher in *Comprehensive Supramolecular Chemistry*, *Vol. 9* (Ed.: J.-M. Lehn), Pergamon, Oxford, **1996**, p. 507.
[132] C. Tedeschi, H. Möhwald, S. Kirstein, *J. Am. Chem. Soc.* **2001**, *123*, 954.
[133] J. H. Fendler, *Membrane Mimetic Chemistry*, Wiley, New York, **1982**.